Nutrient Transporter Inhibition Disrupts Mammary and Intestinal Polarized Epithelial Function

A Thesis Submitted to the
College of Graduate Studies and Research
in Partial Fulfillment of the Requirements
for the Degree of Master of Science
in the College of Pharmacy and Nutrition
University of Saskatchewan
Saskatoon

ABSTRACT

The transporters primarily responsible for transporting important nutrients involved in energy metabolism have a wide substrate specificity setting up the potential for drug-nutrient transporter interactions. Pharmacological inhibition of nutrient transport across the lactating mammary and neonatal intestinal epithelial barrier can directly and indirectly affect growth and maturation of the developing neonate by either reducing the uptake of important nutrients by the neonate or by disrupting epithelial barrier integrity. My thesis focused on two transporters, OCTN2 and MCT1, expressed in immortalized intestinal and mammary epithelial cell cultures to assess the effects of their pharmacological inhibition on L-carnitine and butyrate flux, respectively, and polarized epithelial barrier integrity.

Human colorectal adenocarcinoma (Caco-2) and bovine mammary (BME-UV) cell lines were grown into monolayers on 12-well tissue culture plates and subsequently exposed to the presence or absence of OCTN2 and MCT1 inhibitors for 6, 12, and 24 hours as well as 7 days. Failure to obtain a polarized mammary monolayer prevented the analysis of the direct effects of nutrient transport inhibition on nutrient flux forcing the focus on the indirect effects. To assess polarized epithelial barrier integrity, transepithelial electrical resistance and Lucifer yellow rejection rates were measured at each time point. No trend was noted between control and treated groups. To assess the acute and chronic effects of pharmacological exposure on polarized epithelial function, a limited appraisal of nutrient transporter expression and cellular homeostasis parameters was conducted. Following exposure at each time point, mRNA expression of OCTN1, OCTN2, MCT1, MCT2 and GADPH were measured using qPCR. Low mRNA yields resulted in an inability to assess transporter expression levels in the epithelial systems. Cellular homeostasis parameters were analyzed using the CellTiter-Glo Luminescent Cell Viability Assay, pH-Xtra Glycolysis Assay and MitoXpress Xtra Oxygen Consumption Assay. These assays measured ATP synthesis, glycolytic flux and cellular respiration, respectively. No significant trend was noted in ATP synthesis between control and treated groups. An upward trend in both glycolytic flux and cellular respiration was noted in treatment with both inhibitors in both cell lines.

Complications in obtaining polarized monolayer forced the focus on the indirect affects, therefore, obtaining and utilizing a more accurate portrayal of the lactating mammary and neonatal intestinal epithelium is critical in answering this research question as both of these systems are highly synthetic and complex. By doing so, a more accurate representation of the effects of pharmacological inhibition of nutrient transporters essential for energy metabolism can be identified.

PERMISSION TO USE

In presenting this thesis/dissertation in partial fulfillment of the requirements for a master degree from the University of Saskatchewan, I agree that the libraries of this University may make it freely available for inspection. I further agree that permission for copying of this thesis/dissertation in any manner, in whole or in part, for scholarly purposes may be granted by the professor or professors who supervised my thesis/dissertation work or, in their absence, by the Head of the Department or the Dean of the College in which my thesis work was done. It is understood that any copying or publication or use of this thesis/dissertation or parts thereof for financial gain shall not be allowed without my written permission. It is also understood that due recognition shall be given to me and to the University of Saskatchewan in any scholarly use which may be made of any material in my thesis/dissertation.

Requests for permission to copy or to make other uses of materials in this thesis/ dissertation in whole or part should be addressed to:

Dean of the College of Pharmacy and Nutrition
University of Saskatchewan
Saskatoon, Saskatchewan S7N 5C9
Canada

OR

Dean of the College of Graduate Studies and Research
University of Saskatchewan
107 Administration Place
Saskatoon, Saskatchewan S7N 5A2
Canada

ACKNOWLEDGEMENTS

I would like to express the utmost gratitude to my supervisor, Dr. Jane Alcorn. You believed in me before I believed in myself, and pushed me when I was ready to give up. You gave more than scientific guidance, you gave life guidance. I am the person and scientist I am today because of you, and for that I am sincerely grateful.

I would also like to thank my advisory committee members, Dr. Meena Sakharkar and Dr. Ed Krol, for their comments and suggestions during the various committee meetings. Also, I would like to thank my external examiner Dr. Pat Krone for his valuable comments and suggestions on my research work. I wish to thank my fellow grad students, in particular, Ahmed Almousa, for their help during this work. A special thank-you to Deb Michel for your endless discussions and advice, it was truly invaluable. Furthermore, I thankfully acknowledge the College of Pharmacy and Nutrition, University of Saskatchewan for their financial support to my studies.

TABLE OF CONTENTS

LIST OF TABLES

LIST OF FIGURES

LIST OF ABBREVIATIONS

ABC	ATP-binding cassette transporter
AJC	Apical junctional complex
ATP	Adenosine triphosphate
BCRP	Breast cancer related protein
BME	Bovine mammary epithelium
BSEP	Bile salt excretory protein
cDNA	Copy of deoxyribonucleic acid
DMEM	Dulbecco's modified Eagle's medium
DMSO	Dimethyl Sulfoxide
ECA	Extracellular acidification
EDTA	Ethylenediaminetetraacetic acid
FBS	Fetal bovine serum
g	Gram
HBSS	Hanks balanced salt solution
HEPES	4-(2-hydroxyethyl)-1-piperazineethanesulfonic acid
IBD	Inflammatory bowel disease
IC_{50}	50% Inhibition concentration
K_m	Michaelis-Menten constant
lrECM	Laminin-Rich Extracellular Matrix
LCFA	Long chain fatty acid
LY	Lucifer yellow
MCT	Monocarboxylate transporter
$MgSO_4$	Magnesium chloride
mL	Milliliter
mM	Millimolar
mRNA	Messenger ribonucleic acid
MRP	Multi-drug resistance protein
nm	Nanometer

nM	Nanomolar
OCTN	Organic cation / carnitine transporter
OCR	Oxygen consumption rate
PBS	Phosphate buffered saline
P-gp	P-glycoprotein
pM	Picomolar
rpm	Revolutions per minute
qPCR	Reverse transcription-polymerase chain reaction
SCFA	Short chain fatty acids
SLC	Solute carrier transporter
sIgA	Secretory Immunoglobulin A
SMCT	Sodium-coupled monocarboxylate transporter
TEER	Transepithelial electrical resistance
T_m	Annealing temperature
µg	Microgram
µM	Micromolar
V_{max}	Maximal transport capacity

1. INTRODUCTION

Maintenance of polarized epithelial barrier integrity is essential to ensure a polarized phenotype as well as vectorial transport across the membrane. Although many factors are required to maintain barrier integrity, essential nutrients are critical to maintain epithelial cell homeostasis. Membrane transporters ensure the availability of a variety of nutrients to the epithelial cell, however, these nutrient transporters also transport drugs and other xenobiotics across the membrane. Consequently, a high potential exists for drug-nutrient transport interactions to occur resulting in a loss of nutrient availability with potential concomitant loss of polarized epithelial function and integrity. Such interactions may have clinical relevance and may also identify another potential toxicological mechanism to explain adverse drug reactions. For example, loss of epithelial function through a decrease in nutrient availability may result in disease pathogenesis as noted in Inflammatory Bowel Disease (IBD), or loss of secretion as seen in the lactating mammary gland. The intestinal and lactating mammary epitheliums are two epithelia whose primary function is to assure nutrient availability and maintenance of health and normal development, yet have differing cellular energy requirements. My thesis research intends to address the consequences of xenobiotic-nutrient transporter interactions with a focus on nutrients essential for energy metabolism within epithelia that rely on different energy metabolism pathways in the hope of identification of a toxicological mechanism of action not generally appreciated in the literature. Furthermore, my thesis research is premised in the ongoing investigations in my lab involving the lactating mother-neonate dyad and the toxicological risk to the nursing neonate following drug/disease interactions in the medicated mother.

My thesis specifically focuses on the essential nutrients, L-carnitine and butyrate. These nutrients are not only required for development of the neonate, but also the maintenance of epithelial barrier integrity and function. The mammary and intestinal epithelium represent complex barriers separating compartments of different compositions and the integrity and proper functioning of these barriers is critical to the provision of adequate nutrition to the neonate. L-Carnitine has an important role in mitochondrial utilization of long chain fatty acids for energy metabolism and butyrate represents an important energy source for colonic cells and is involved

in epigenetic regulation. Both nutrients require carrier mediated transport into the epithelial cell and adequate cellular availability of these nutrients is critical to ensure proper barrier integrity and the maintenance of polarized epithelial function. Furthermore, the transporters involved in the uptake of L-carnitine and butyrate also include in their substrate profiles numerous xenobiotics. This creates a potential for significant drug-nutrient transporter interactions to occur. Therefore, in my thesis I evaluate the inhibition of transporter mediated uptake of the essential nutrients, butyrate and L-carnitine, and the effects on epithelial barrier integrity as a proof of concept investigation to represent the plausible effects that can occur in the medicated nursing mother-neonate dyad, i.e. loss of epithelial barrier integrity and function of the intestine and/or mammary gland can have detrimental effects on the provision of nutrition to the neonate and overall neonatal health and development.

2. LITERATURE REVIEW

2.1 Lactating Mother-Neonate Dyad

Following birth, neonates are required to rapidly adjust from the intrauterine to the extrauterine environment. One of the major adaptations required is the switch of nutrition from umbilical blood to milk supplied from the lactating mother. This sets up a complex and dynamic unit and interchange between the mother and child to allow the neonate to receive the essential nutrients required for proper growth and development. In the exclusively breastfed neonate, the mammary epithelium must assure adequate availability of all essential nutrients while the neonatal intestinal system must function adequately to absorb these essential nutrients for appropriate growth and maintenance of neonatal health. Any disruption to the availability of nutrients by the maternal mammary gland or the absorbance of the nutrients at the neonatal intestinal gland may adversely impact the health and development of the breastfeeding neonate.

2.2 Importance of Breastfeeding

Breastmilk is the biological and natural way to feed infants versus the synthetic substitute of formula. Exclusive breastmilk feeding for the first 6 months of life, with continued feeding for 1-2 years has become the recognized standard for infant feeding (1). Breastmilk has many benefits over its formula substitute including containing the essential components required by the neonate to adapt to the post-natal world. Breastmilk contains a number of nutrients required for growth and development and also provides protection from infections and immune mediated disease and also allows the infant's own immune system to mature (2). The majority of diseases with an immune component in their etiology have a lower incidence rate in breastfed infants compared to formula fed infants (3). Further, breastmilk's functional components uniquely adapt to the changing needs of the neonate to support growth making it far superior to formula.

2.2.1 Changes in Milk Composition with Time to Meet Neonate Requirements

Human milk is a complex fluid that uniquely adapts to the needs of the developing neonate. After parturition, the requirements of the neonate are constantly shifting and the components of milk mirror that shift with changes to meet these requirements. The initial milk to be secreted, colostrum, is produced in low quantities and is predominated by growth factors and

immune protective proteins due to the neonate's naïve and immature immune system. Colostrum also contains low concentrations of lactose representing it's primary function as immunologic rather than nutritional (1). As lactation continues, the concentration of these proteins decreases, and casein (source of amino acids), increases (3).

The first notable change to occur in the milk composition following parturition is an increase in lactose concentration and a decrease in sodium and chloride concentrations (4). This comes following the closure of tight junctions of the mammary epithelium to allow the volume of milk to grow within the lactiferous ducts. With the closure of the tight junctions at the mammary gland epithelium, lactose can no longer pass between the epithelial cells into the maternal blood, and sodium and chloride can no longer pass from the interstitial space into the lumen of the gland. The next change noted is an increase in the concentration of protective proteins, such as secretory immunoglobulin A (sIgA) and lactoferrin (5). The concentration of these proteins remain high for 2 days postpartum and then decrease rapidly due to dilution by the increased volume of secreted milk (5). The increase in milk secretion is also accompanied by an increase in the rates of synthesis and secretion of the majority of milk components including lactose, casein, calcium, sodium, magnesium and potassium (6). This allows the milk to provide nutrients with high bioavailability and in sufficient quantities to support the growing needs of the developing neonate.

The nutritional components of human milk, either macronutrients or micronutrients, derive from 3 sources: synthesis in the lactocyte, dietary, and from maternal stores (1). Macronutrient composition is conserved compared to micronutrients, however, can differ between preterm and term milk with preterm milk being higher in protein and fat (1). The proteins in human milk are divided into two fractions, whey and casein, each with a specific array of proteins and peptides with the most abundant being casein, α-lactalbumin, lactoferrin, sIgA and lysozyme (7). Fat is the most variable macronutrient and is characterized by high contents of palmitic and oleic acids in varying positions of the triglycerides (1). The primary sugar found in human milk is disaccharide lactose and is the least variable in concentration among the macronutrients (8). The micronutrients in human milk, including vitamins A, B1, B2, B6, B12, and D, and iodine, are far more variable and may depend on maternal diet and body stores (1)

Concentrations of certain micronutrients, including L-carnitine, have been shown to vary over the course of lactation correlating to the changing expression of transporters. Our laboratory

challenged L-carnitine transporters with inflammatory agents and noted an increase in maximal activity (V_{max}) of L-carnitine transport without an effect on the affinity (K_m). This corresponded to changes in mRNA expression of the OCTN2 transporter (previously reported in our laboratory) and to changes in cellular energy levels and oxygen consumption rates (Uma Manthena MSc Thesis).

Changes in transporter expression has been shown to vary depending on the duration of lactation corresponding with the needs of the developing neonate at that time (9, 10). Five distinct patterns have been shown: 1) decreasing throughout lactation (OCTN2), 2) prominent increase in early lactation, which may remain elevated or decline with advancing lactation (OCTN1), 3) constant but decreasing later in lactation (OCTN3), 4) increasing until mid-to-late lactation (OCTN1), 5) prominent increase late in lactation (Ncbt1) (10). The varying expression of OCTNs allow for a greater drug-nutrient interaction involving L-carnitine resulting in significant differences in milk-serum ratios of L-carnitine (9).

2.2.2 Role of Milk in Neonatal Health

Neonates are developmentally immature at birth and rely solely on the mother's milk supply to aid them in the transition to the post-natal world. The complex fluid is an intrinsic mixture of bioactive proteins, lipids and carbohydrates that allows for the stimulation of cellular growth, digestive maturation, establishment of symbiotic microflora, and the development of gut lymphoid tissues (3).

The nutritional composition in human milk, both macronutrients and micronutrients, are designed for host defense, antimicrobial protection, and stimulation of immunocompetence (3). Lactoferrin, a major protein found in breast milk, chelates free iron increasing the rate of absorption of iron by the infant. This key protein also inhibits the pathobiology of several bacteria (11), stimulates phagocytosis of pathogens (12), and inhibits human immunodeficiency virus (13). The large fat (triglyceride) content in breast milk also aids in development. Upon digestion, the triglycerides are converted into free fatty acids and monoglycerides which inhibit viruses, some bacteria and protozoans (14). IgA exists in concentrations around 1 g/L in breast milk and helps with the inhibition of infection by enteric pathogens (15). This antibody is not digested fully allowing accumulation in the intestine to occur where it binds to antigens rendering the pathogen less infective (15).

Beyond maturation of the GI tract, the multifunctional role of breast milk provides the tools for the successful development of the neonate. The lipids in the breast milk are vital for neonatal growth and development as they provide a dense energy source as well as essential fatty acids such as docosahexaenoic acid (DHA) (16). Though various lipids are the major energy-yielding substrates in breast milk, carbohydrates also provide energy for the newborn, and are essential for central nervous system kidney, brain, muscle (including the heart) function (17). The micronutrients can modify hormones, growth factors and cell signaling pathways, with subsequent effects on development during early life (18). For example, milk contains erythropoietin (Epo), the primary hormone responsible for increasing red blood cells (RBCs). This is critical as blood loss, intestinal pathology, and immaturity of the hematopoietic system contribute to anemia in premature infants, which can drastically affect growth and development (1).

2.3 Role of Mammary and Intestinal Epithelium in Neonatal Nutrition

The mammary and neonatal epithelial systems work in concert to ensure the neonate receives proper nutrition. The mammary gland, through a process called lactogenesis, becomes sufficiently differentiated to synthesize and secrete milk. With nursing, the intestinal epithelium of the neonate is responsible for the absorption of the essential nutrients found within the milk that are critical for the proper growth and development of the neonate. Both the availability of the nutrients to the lactating mammary epithelium and the absorption of nutrients at the intestinal epithelium rely on a proper functioning epithelial system.

The main role of the polarized epithelium is to act as a selective barrier that regulates the composition of opposing compartments and to maintain homeostasis. Achievement of these functions is dependent upon a surface membrane that is organized into structurally, biochemically and physiologically distinct domains (apical and basolateral) containing specific ion channels and transport proteins (19). Epithelial cell membranes compose the majority of the barrier and are largely impermeable to hydrophilic solutes except where transporters are present. The domain facing the luminal compartment, the apical domain, is lined with specialized proteins that depict the main function of the cell (ie: absorption or secretion) (19). The basolateral membrane faces the extracellular compartment and contacts adjacent cells and has specialized junctions as well as cell adhesion structures (20). These junctional complexes are

essential in the role of maintaining a polarized phenotype within the epithelial cells and ensuring vectorial transport across the membrane (19, 20).

The apical junctional complex (AJC) allows for the separation of the apical and basolateral domains and is an essential signaling center critical to the function of the polarized epithelium (20). Tight junctions, a particularly important part of the AJC, create the barrier between the apical and basolateral surface as well as between adjacent cells limiting paracellular transport and promoting transcellular transport. Transcellular transport from one side of the epithelium to the other occurs mainly through passive diffusion and carrier mediated transport but can also be the result of endocytosis and exocytosis (together coined transcytosis). Transport via this mechanism is directional, energy dependent, and governed by cell-specific transporters and channels positioned either on the apical or basolateral membrane (21) and is also the primary route that nutrients transverse the epithelial barrier.

Proper function of the polarized epithelium is critical to regulate the compositions of the luminal and extracellular compartments. If barrier integrity of the epithelium becomes compromised, paracellular transport will become more prominent leading to altered composition of the opposing compartments resulting in a disruption in homeostasis. Due to the highly regulated and synthetic nature of these two epithelial systems, any disruption to cellular energy homeostasis can, in turn, lead to impaired barrier integrity. In particular, adenosine triphosphate (ATP) synthesis and oxygen consumption are two factors that are critical for the regulation of cellular energy homeostasis and the maintenance of the mammary and intestinal epithelial barrier (22).

2.3.1 Lactating Mammary Epithelium

The lactating mammary gland is a complex network of ducts formed of epithelial cells ending in lubulo-alveolar clusters, which are ultimately the site of milk secretion (23). Each alveolus is surrounded by a monolayer of polarized epithelial cells which is in turn surrounded by myoepithelial cells that aid in the function of milk secretion (23). The mammary epithelium is responsible for the synthesis of or availability of many of the milk constituents, making it one of the most highly synthetic tissues of the body. Due to the high activity of these cells, a large amount of energy is required. The main metabolic pathway utilized by the lactating mammary

gland is glycolysis; the conversion of glucose into pyruvate allowing free energy in the form of ATP to be released (24).

2.3.1.1 Lactogenesis

Lactogenesis, the initiation of lactation, is a complex process that represents numerous changes in the activity of differentiated mammary epithelial cells from inactive non-secretory state to an active secretory state (25). Lactogenesis begins around mid-pregnancy in most species, including humans, and has been divided into two phases: Initiation phase and activation phase based on differences in the composition of the secretions, expression of genes, and structural and functional properties of the cells (23, 26)

The initiation phase (lactogenesis I) occurs during pregnancy when the mammary gland becomes sufficiently differentiated allowing the alveolar cells the capability to secrete small amounts of specific milk components including α-lactalbumin and lactose, which in humans, can be detected in the plasma and urine (27) This stage of lactation is characterized by an increased expression of milk protein genes, biosynthetic enzymes, as well as an accumulation of neutral lipid droplets (26). The mammary gland is sufficiently differentiated to secrete milk following completion of this phase, but milk secretion is prevented by high plasma concentrations of progesterone (28).

Copious secretion of milk occurs during the activation phase of differentiation (lactogenesis II) which after parturition in humans (23). This phase is characterized by induction of additional milk protein genes and enzyme expression, polarization of organelles, expansion of mitochondria and rough endoplasmic reticulum, and maturation of the Golgi apparatus (26, 29). These drastic changes, accompanied by the closure of the tight junctions, occurs during the first 4 days following birth allowing the infant to receive 500-750 mL of milk per day by day 5 (6).

The secretion during lactation is a complex mixture coming from different secretory pathways across, within, and also between mammary epithelial cells (30). There are five major routes of secretion across the lactating mammary epithelium from the blood side to milk, four transcellular and one paracellular: *1)* membrane route, *2)* golgi route, *3)* milk fat route, *4)* transcytosis, and *5)* paracellular route (31). Transport across the lactating mammary epithelium is mainly attributed to transcellular transport, however, there are times when a significant flux occurs via the paracellular route such as during pregnancy (30).

2.3.2 Intestinal Epithelium

The intestinal epithelium is the largest mucosal surface in the human body with the key job of protecting an individual from the external environment and providing nutrients to sustain life (32). The epithelium forms a selectively permeable barrier that separates contents of the intestinal lumen from the interstitium while maintaining body homeostasis (33). The epithelial cells form an effective barrier to the majority of hydrophilic solutes, however, the paracellular space must also be considered for an intact barrier (33). Paracellular permeability of the intestinal epithelium depends on the dynamic regulation of tight junctions. Due to the diverse challenges the intestinal epithelial barrier is subjected to, the tight junctions must be capable of rapid and complex responses (32).

Due to the complex and active nature of the intestinal epithelium, high amounts of energy are required. The main energy source for colonic cells is β-oxidation of short chain fatty acids derived from bacterial carbohydrate fermentation (34). Acetate, propionate, and butyrate are the three main acids with butyrate being the preferred fuel accounting for about 70% of total energy consumption (34). Absorption of short chain fatty acids across the apical membrane is concentration dependent with no saturation and is coupled with sodium absorption (35). Much like the mammary gland, the small intestine makes use of glucose for energy requirements (36). Primarily, glucose is utilized via the glycolytic pathway with less than 5% of the glucose utilization occurring via the pentose phosphate pathway (36).

2.3.2.1 Neonate's Intestine

At the time of birth, the neonate's gastrointestinal (GI) tract is underdeveloped and immature. Following parturition, there is a period of drastic changes in the neonate's GI tract. Mucosal immunity begins to develop in utero and continues from birth to early childhood. The intestine undergoes significant growth and adaptation to exogenous and endogenous stimuli in response to feeding (37). Nutritional components as well as stimuli from the microenvironment, including the gut microbiome, help to regulate and develop the immune response within the intestine (37). Human milk is designed to aid in host defense, antimicrobial protection, and stimulation of immunocompetence (3). Breast milk feeding allows the neonatal intestine to be exposed to the protective anti-inflammatory nutrients required until the developing infant can synthesize its own anti-inflammatory mechanisms (2).

2.4 Nutrients

Numerous nutrients are required for the proper development of the neonate and maintenance of normal body function. Some nutrients, however, are more critical than others and can, therefore, be divided into three categories: essential, conditionally essential, and non-essential. The essentiality of a nutrient signifies that is has an indispensable physiological function, and when withdrawn from the diet, results in implications in growth and development and sometimes illness (38). An essential nutrient cannot by synthesized endogenously at an adequate rate by a healthy individual and, therefore, must be received by diet (38). A nutrient is considered 'conditionally essential' when there is a critical physiological function and it is nutritionally nonessential for normal subjects, however, synthesis is rate-limited (such as in the immature neonate) or lost in certain individuals (38, 39). Nutritionally nonessential nutrients can also serve key physiological functions but they can be synthesized at a sufficient rate such that dietary withdrawal causes no adverse effects (38).

2.5 Carrier-Mediated Transport of Nutrients across the Epithelium

The majority of nutrients utilize carrier-mediated transport to transverse the epithelia. This transcellular mechanism makes use of membrane proteins that act as vectorial transporters across the epithelium. Compared to passive diffusion, much greater levels of transport are achieved through carrier-mediated mechanisms. Unlike passive diffusion, a carrier-mediated mechanism is subject to saturation as well as inhibition. Inhibition, a result of a competitive or non-competitive interaction with another compound, has the potential to prevent the transport of the desired compound. This can lead to a disruption in the cellular homeostasis inadvertently leading to a disruption in barrier integrity.

Transporters can generally be divided into two classifications; uptake transporters and efflux transporters, with both being essential for the maintenance of homeostasis and barrier integrity. Uptake transporters are required for the cellular entry of compounds and are generally noted by members of the solute carrier (SLC) super family of transporters (40). Efflux transporters require energy to export compounds out of the cell due to the transport often being against a concentration gradient (40). The majority of efflux transporters are members of the ATP-binding cassette (ABC) superfamily and utilize binding and hydrolysis of ATP to function and mediate transport (40). To fully understand the disposition of nutrients, consideration of the

complex interplay between uptake and efflux transporters within a given epithelium must be given due to the possibility of nutrient movement being either impeded or facilitated by the existence and localization of transporter proteins at either domain (40).

2.5.1 ATP-Binding Cassette Transporter Superfamily

The ATP-Binding Cassette (ABC) superfamily has been divided into seven sub-families with 49 known human ABC genes, 48 which are functional (41). ABC Transporters are mainly responsible for the efflux of substrates via an active, ATP-dependent manner against dynamic concentration gradients (42). This family of transporters contain a pair of ATP-binding domains (nucleotide binding folds (NBFs)), and two sets of transmembrane domains, and typically contain six membrane-spanning α-helices (43). The localization of these transporters is primarily in the plasma membrane, where they export a variety or structurally diverse drugs, conjugates and metabolites as well as other compounds from the cell (42). Members of the ABC transporter family have become a critical defense mechanism limiting exposure to cells to toxic xenobiotics (40). These efflux transporters account for the removal of a wide variety of compounds including phospholipids, steroids, polysaccharides, peptides, amino acids, ions, organic anions, bile acids, drugs and other xenobiotics (41)

There are three classes of ABC transporters; P-glycoprotein (P-gp; ABCB) family, multidrug-resistance associated (MRP; ABCC) protein family, and the breast cancer resistance (BCRP; ABCG) protein family (40). The P-gp transporters consist of two similar halves, each containing six transmembrane segments and an intracellular ATP binding site (42). MRP transporters have a similar architecture at the P-gp family with the addition of an N-terminal extension (42). The BCRP transporter family is the most recently discovered, and unlike the others, is a half transporter with only a single N-terminal, intracellular ATP binding site, and six transmembrane segments (42).

2.5.2 Solute Carrier Transporter Superfamily

The Solute Carrier (SLC) transporter superfamily is by far the largest group of transporters with 55 sub-families with at least 362 known SLC genes with 20-25% amino acid sequence shared by member proteins belonging to the same SLC gene family (44). Members of this transporter superfamily have varied biochemical properties and include passive transporters,

active transporters, as well as mitochondrial and vesicular transporters (44). Active transporters couple the movement of one molecule against its concentration gradient, to the gradient of another molecule, while passive transporters only transfer molecules along their own concentration gradient (44, 45). Localization within the cell varies depending on the type of transporter being considered. The majority of SLC transporters are localized to the plasma membrane while others are located in the mitochondria (46), peroxisomes (47), and synaptic vesicles (48).

2.5.2.1 Organic Cation-Carnitine Transporters

Organic Cation-Carnitine Transporters (OCTNs) belong to the SLC22A family of transporters and are widely expressed in mammalian tissues. Three types of OCTNs have been identified; OCTN1, OCTN2, and OCTN3. The first discovered, OCTN1, showed similar structure to organic cation transporters (OCTs) and organic anion transporters (OATs), and transports organic cations (49). The second member, OCTN2, is a Na^{2+}-dependent transporter and has the ability to interact with a variety of cations including L-carnitine, an essential nutrient involved in β-oxidation of long chain fatty acids (50). This transporter is critical for the movement of L-carnitine as it is the primary transporter that mediates the Na^{2+}-independent transport of this essential nutrient (51). OCTN2 has been identified as the gene responsible for inherited primary systemic L-carnitine deficiency as it is essential for the reabsorption of L-carnitine that has been filtered through the glomerulus across renal epithelial cells (52). OCTN3, the third member of the family, has specific activity for L-carnitine only (53). The OCTNs, although very similar in amino acid sequences, have distinct functional binding sites allowing them to discriminate against other substrates. However, OCTN2 may have multiple universal binding sites as it accepts both L-carnitine and other organic cations (53).

2.5.2.2 Monocarboxylate Transporters

Monocarboxylate Transporters, responsible for the uptake of monocarboxylates into epithelial cells, can be classified into two types; proton-coupled monocarboxylate transporters (MCTs) and Na^{2+}-coupled monocarboxylate transporters (SMCTs). There are 14 members of the MCTs (MCT1-14) which belong to the SLC16A family of transporters. The MCTs are responsible for the transport of short-chain monocarboxylates such as lactate, pyruvate, and

butyrate for production of long chain fatty acids. Further, and more critical, MCT1 transports ketone bodies and SCFAs from cell cytosol to mitochondria for the production of cellular metabolic energy (54). MCT1 has been shown to be the primary transporter for butyrate, a short chain fatty acid responsible for up to 70% of colonic energy supplies (54). Any alteration in the expression of MCT1 would decrease the intracellular availability of butyrate drastically affecting cell regulatory effects (55).

2.6 Drug-Nutrient Transporter Interactions

Drug-nutrient transporter interactions are defined as any physical, chemical, physiologic, or pathophysiologic relationship between a drug and a nutrient transporter (56). Drug induced inhibition of nutrient transporters, such as MCT1 and OCTN2, is increasingly being recognized as an important toxicological mechanism due to the severe consequences related to such interactions (9, 57). This is exemplified by the recent identification of inhibition of bile salt excretory protein (BSEP) as a significant cause of drug induced liver injury (58). Numerous drugs can interfere with normal bile formation resulting in cholestasis in the mammalian liver which is characterized by pruritus, jaundice caused by hyperbilirubinemia, altered lipid and cholesterol metabolism, and intestinal malabsorption of fat and fat soluble vitamins (58). Chronic conditions result in biliary cirrhosis due to bile salt-induced toxic liver cell necrosis leading to fibrosis and cirrhosis (58). Due to the serious adverse effects associated with BSEP inhibition, several drugs have been withdrawn from the market leading to the inclusion of BSEP inhibition potential by the Pharmaceutical Industry in their drug discovery toxicological screening assays.

Inhibition of nutrient transporters has the potential to decrease nutrient availability to the epithelium and, in turn, result in the epithelium not operating optimally. Without proper management or recognition, these interactions may lead to treatment failure, toxicity and sometimes fatal adverse effects. This is especially exemplified when considering the inhibition of essential nutrients that are required by the developing neonate. Due to the many substrates associated with key nutrient transporters there is a high potential for drug-nutrient interactions to occur that may have clinical relevance. Drug-nutrient interactions have been well documented in many systems including the GI tract, kidney and liver while some areas, including the mammary gland, have received limited attention (59).

2.6.1 Interactions at the Mammary Epithelium

Interactions at the lactating mammary epithelium has the potential to lead to numerous adverse effects including the disruption of milk volume and composition, affecting the blood flow to the mammary gland, or through direct/indirect interference with nutrient secretion (60). Nutrient secretion across the mammary epithelium into the milk space is essential as the milk is often the sole source of many nutrients required by the developing neonate. Any disruption to nutrient secretion across the epithelium, therefore, could be detrimental as it would impede on proper development. Numerous transporter families expressed in the mammary gland during lactation are responsible for the transport of both nutrients and non-nutrient elements including various drugs setting up the high potential for interactions to occur (61). Despite this, drug-nutrient transporter interactions at the mammary epithelium and the consequences of said interactions have received very limited attention.

Recent studies in our laboratory have shown an important drug-nutrient transport interaction at the mammary gland involving L-carnitine, a conditionally essential nutrient required by the neonate for proper development. Several transporters mediate the transport of L-carnitine, namely the OCTN transporters, however, substrates of these transporters also include cationic drugs such as verapamil, valproate, and the β-lactam antibiotics, cephaloridine and cefepime (62). When administered, cefepime significantly reduced the milk concentration of L-carnitine in early lactation (day 4), theoretically, through an interaction with OCTN2 (9).

Further analysis of interactions at the mammary epithelium is absolutely critical due to the potential for serious adverse effects to occur. The developing neonate is in a sensitive state, therefore, any maternal factor (e.g. disease, diet, exposure to xenobiotics) that adversely alters breast milk composition could reflect negatively on the proper development on the infant (63). Yet, drug-nutrient transporter interactions at the lactating mammary epithelium represent a fundamental knowledge gap that desperately needs to be filled.

2.6.2 Interactions at the Intestinal Epithelium

Drug-nutrient interactions have been extensively studied and well documented in the GI tract. Primarily, intestinal transporters are responsible for the absorption of molecules that are produced during digestion of food; however, they additionally are an important site of secretion of many substrates via efflux transporters (59). With the high degree of absorbance and

secretion, there is a high chance of an interaction occurring between essential nutrients and other substrates including drugs. Disruptions of nutrient availability in the GI tract through these interactions have the potential to lead to adverse effects including pathogenesis. This is exemplified in the case of IBD where there is an impairment of butyrate metabolism and L-carnitine availability and a switch to glucose utilization due, in part, to downregulation and/or loss of function of the butyrate transporter, MCT1, and high affinity L-carnitine transporter, OCTN2 (64).

Numerous substrates have been shown to inhibit the transporter MCT-1 in the GI tract. A key interaction that has been documented involves the compound α-cyano-4-hydroxycinnamate (4-CIN), which has the potential to competitively inhibit MCT-1 in human colonic cancer cells (65). This is of particular concern as MCT1 is the primary transporter involved in the transporter of butyrate, the main energy source for colonic cells. Further, this compound inhibits the entry of pyruvate into mitochondria and prevents the subsequent metabolism of pyruvate derived from glucose potentially having effects on energy metabolism through the tricarboxylic acid cycle (TCA cycle) (66). Any disruption in the availability of butyrate is of concern due to the impacts on cell homeostasis.

2.7 Two Transported Nutrients Important in Epithelial Energy Metabolism: L-Carnitine and Butyrate

2.7.1 L-Carnitine

L-Carnitine is a water soluble molecule that is conditionally essential in neonates as L-carnitine biosynthesis is developmentally immature and neonates, therefore, rely solely on maternal sources through breast milk to meet their needs (9, 67). This nutrient is critical for the proper development of the cardiovascular and neurological systems in all nursing neonates (68). L-Carnitine is essential for the utilization of long chain fatty acids (LCFAs) as it facilitates the transport into the mitochondrial matrix (69). Oxidation of LCFAs is necessary for the normal development and survival of the developing neonate (69). All enzymes required for β-oxidation of LCFAs are located within the matrix and, therefore, there must be adequate concentrations of L-carnitine in the tissues or β-oxidation will decrease and cellular energy metabolism impaired (69). L-Carnitine serves other physiological roles in the body including activation of aerobic

glycolysis, enhancement of respiratory chain function, donor of acetyl groups for biosynthesis (e.g. acetyl choline) and membrane stabilization (68).

With the many functions of L-carnitine, a deficiency can result in severe and even lethal consequences. Since L-carnitine is critical for the production of energy for many organs, deficiencies have been associated with cardiomyopathy, muscle weakness, encephalopathy and/or hepatopathy including Reyes syndrome (70). Further, deficiencies in L-carnitine have been related to limb girdle myopathy, failure to thrive and recurrent hypoketotic, hypoglycemic coma and seizures which have the potential to be lethal (71). However, the majority of symptoms are reversible with high-dose life-long oral L-carnitine supplementation (71).

Several transporters mediate the transport of L-carnitine including organic cation/carnitine transporters (OCTN1, OCTN2 and OCTN3) (9). Total concentration of L-carnitine in human tissues is highest in the heart and skeletal muscle, as opposed to the liver and brain, which reflects the higher rate of LCFA oxidation that occurs in these tissues (72). Initial concentrations of L-carnitine in the neonate directly depend on the maternal concentrations as neonates lack the ability to synthesize their own L-carnitine (73). Plasma concentrations of this conditionally essential nutrient increases during the first two weeks of life and reach adult levels by six months following parturition (74).

2.7.2 Butyrate

Butyrate, a short chain fatty acid (SCFA), plays an important role in maintaining the health and integrity of the colonic mucosa (55). Butyrate, acetate, and propionate, the predominant SCFAs, are absorbed readily by colonocytes and are used as the preferred source of fuel by these cells (75). Butyrate is oxidized more readily than propionate and acetate by colonocytes and its oxidation occurs regardless of the presence of other SCFAs (76). Due to this, β-oxidation of butyrate accounts for up to 70% of the totally energy consumed by the colonocytes (77). Further, butyrate promotes proliferation and differentiation of colonic epithelial cells, modulates the proliferative potential of cultured human colon tumour cell lines (78) as well as involved in the activation of several differentiation-specific genes (79, 80). At colonic pH, SCFAs exist almost entirely as anions and require a carrier protein for cellular entry (81). Transport of butyrate across the apical membrane involves the monocarboxylate transporter family, specifically, MCT1 (54, 82). Therefore, any modulation to the expression of MCT1

would reduce the intracellular availability of butyrate, disrupting not only cell energy metabolism but cell regulatory effects (55).

2.8 Hypothesis and Objectives

Transport of essential nutrients across the mammary and intestinal epithelium is achieved by nutrient transporters. However, these transporters' substrate profile includes numerous xenobiotics as well as the nutrients setting up the potential for drug-nutrient transporter interactions to occur. Any disruption to the availability of nutrients by the maternal mammary gland or the absorbance of the nutrients at the neonatal intestinal gland may adversely impact the health and development of the breastfeeding neonate, in particular, through altered cellular homeostasis. Therefore, we evaluated the inhibition of nutrient-transporter mediated uptake of important nutrients required for the maintenance of cellular homeostasis. This will be used as a proof of concept to represent the plausible effects that can occur to the mother-neonate dyad when the mother requires medication while nursing her infant.

2.8.1 Hypothesis

Inhibition of L-carnitine or butyrate transport disrupts epithelial barrier integrity through a reduction in cellular energy metabolism and loss of tight junction function.

2.8.1.1 Objective I

Assess the acute and chronic effects of L-carnitine and butyrate transport inhibition on the integrity of the intestinal and mammary epithelium by measuring transepithelial electrical resistance (TEER), Lucifer Yellow rejection rates, and transporter expression.

2.8.1.2 Objective II

Assess the acute and chronic effects of L-carnitine and butyrate transport inhibition in mammary epithelial and GI epithelial barriers on cellular energy metabolism by measuring cellular respiration, glycolysis rate, and cellular ATP.

3. MATERIALS AND METHODS

3.1 Chemicals, Reagents, Kits, and Cell Culture Materials

Caco-2 intestinal cell line was purchased from American Tissue Culture Collection (Rockville, MD) and the Bovine Mammary Epithelium cell line was a generous gift from Dr. Bruce Schultz from Kansas State University, Manhatten, KS, USA. T-75 flasks, sterile 15 mL and 50 mL polypropylene centrifuge tubes, 96 well plates, eppendorf tubes, NCTC-135 cell culture media, Fetal Bovine Serum (FBS), Newborn Calf Serum (NCS), Iron Supplemented Bovine Calf Serum (FeBCS), Insulin-transferrin-sodium selenite, and SuperScript VILO cDNA Synthesis Kit were purchased from Thermo Fisher Scientific (Ottawa, Ontario, Canada. Dulbecco's Modified Eagle's Medium (DMEM), Ham's F-12 medium (DMEM-F12), and RPMI-1640 cell culture medium as well as dimethyl sulfoxide (DMSO) was purchased from American Type Culture Collection (ATCC) (Rockville, Maryland, USA). Corning® HTS Transwell-24 well permeable supports, Calcein-AM kit, and Lucifer Yellow were purchased from Sigma-Aldrich (Oakville, Ontario). Verapamil was purchased from Cayman Chemical Company, CAS No. 152-11-4 (Michigan, USA). AR-C155858 was purchased from Tocris Bioscience, CAS No. 4960 (Bristol, UK). Ribonucleic acid (RNA) isolation midi kit was purchased from Qiagen Inc. (Toronto, Ontario, Canada). Quantitative reverse transcription-polymerase chain reaction (qPCR) tubes and one-step SYBR green RT-PCR kits were acquired from Applied Biosystems (Foster City, California, USA). CellTiter-Glo Luminescent Cell Viability Assay was purchased from Promega (Madison Wisconsin, USA). MitoXpress Xtra Oxygen Consumption Assay and pH-Xtra Glycolysis Assay was purchased from Luxcel Biosciencs (Cork, Ireland). Highly purified deionized water was obtained from a MilliQ Synthesis water purification system (Millipore, Bedford, MA). All other solvents and reagents used were of the highest analytical grade available.

3.2 Cell Lines

For all experiments, we made use of the Caco-2 (human colorectal adenocarcinoma) and BME-UV (bovine mammary) polarized epithelial cell lines as both of these *in vitro* models have functional and morphological characteristics that mimic the *in vivo* system. Although the Caco-2 cell line is not neonatal in origin, it served as a substitute for this proof of concept study. Caco-2

polarized epithelial cells have routinely been cultivated into monolayers to study transepithelial transport of drugs across the intestinal epithelium (83). BME-UV polarized epithelial cell line is a newer model that has been shown to form a confluent, polarized monolayer capable of regulated ion transport allowing the characterization of the mammary epithelium (84). Further, both Caco-2 and BME-UV cells lines express the transporters involved in the high affinity transport of L-carnitine and butyrate into epithelial cells, namely OCTN2 and MCT1, respectively (85, 86).

3.2.1 Caco-2

Caco-2 cells were cultured under conditions similar to those described previously (83). The cells were grown in DMEM supplemented with 10% fetal bovine serum (FBS) and 1% antibiotic solution (10,000 units penicillin, 10 mg/mL streptomycin) in T-75 flasks. The media was changed every second day. Cells were passaged at 70% confluency twice after removal from liquid nitrogen. Passage of cells in the flasks were performed by aspirating spent medium from the flask, rinsing with Trypsin (0.25% in phosphate-buffered saline; PBS) containing 0.2% EDTA to neutralize the FBS, and then incubated with 5 mL of Trypsin for 5 minutes to allow the cells to detach. Ten mL of media (DMEM with 10% FBS and 1% antibiotics) was added to stop the Trypsin and the total suspension was added to a 15 mL centrifuge tube and centrifuged for 5 mins at 1000 rpm. Media was aspirated and the cell pellet was re-suspended in 10 mL of fresh media.

3.2.2 BME-UV

BME-UV cells were cultured under conditions similar to those described previously (87). Cells were cultured in Typical Bovine Media (Table 3.1) in T-75 flasks. Before use, all media was supplemented with 1% insulin-transferrin-sodium selenite and 1% penicillin-streptomycin and pH adjusted to 7.4. Passaging was performed the same as with Caco-2 cells.

Table 3.1: Typical Bovine Media Composition

Component	Amount
Dulbecco's Modified Eagle Media (DMEM)	21.25%
Ham F-12 nutrient mixture (F-12)	21.25%

RPMI-1640	25.50%
NCTC-135	17%
Fetal Bovine Serum (FBS)	10%
Newborn Calf Serum (NCS)	3%
Iron-supplemented Bovine Calf Serum (FeBCS)	2%
Lactalbumin Hydrosylate	1 mg/mL
L-Ascorbic	10 μg/mL
Lactose	2 mM

*Before use, all media was supplemented with 1% insulin-transferrin-sodium selenite and 1% penicillin-streptomycin. Media was made in 500 mL increments and pH adjusted to 7.3, filter-sterilized with 0.22 μm filters and stored in opaque bottles at 4°C.

3.3 Optimization Studies to Identify Inhibitor Concentration

Optimization studies were performed to determine nontoxic concentration ranges of the proposed transport inhibitors for subsequent studies and made use of the Calcein-AM kit. Cells were seeded onto 96-well plates at a density of 10,000 cells/288 μL per well. The cells were allowed 24 hours to attach, and then were exposed to a serial dilution range of the transporter inhibitors (Verapamil concentration range from 10 nM-10 mM and AR-C155858 concentration range from 6.5 pM-6.5 μM made in 1% DMSO diluted in media). The solvents were made by plating 100% DMSO at 100x the concentration as needed. 22 μL of the 100% DMSO samples were added to 198 μL of media to create a 10% DMSO solvent. 32 μL of the 10% DMSO solvent was added to the seeded plate containing 288 μL of media creating 1% DMSO concentration. Wells were also treated with the vehicle mixture of 1% DMSO to ensure no cytotoxicity occurred and to give background readings as well as 5-Flurouracil (also dissolved in 1% DMSO) as a positive control. Cells were treated and allowed to incubate for 72 hours at 37°C and 5% CO_2. Following incubation, spent media was aspirated and cells were washed with Calcein washing buffer, followed by the addition of 100 μL of Calcein working solution (10 μL of 2 mM Calcein added to 10 mL PBS) and incubated for 30 minutes at 37°C and 5% CO_2. Following incubation, the fluorescence was read at 485/530 nm. IC_{50} values were calculated on GraphPad Prism 5 (San Diego, California, USA) with nonlinear regression.

3.4 Assessing Barrier Integrity

On three separate occasions, cells were seeded at a density of $1x10^5$ cells/well on polyester membrane transwells (Figure 3.1) in the apical compartment (inserts measure 24 mm in diameter and have a pore size of 0.4 µm). Both cell lines were washed and new media was added every two days for three weeks. Initial TEER measurements were obtained using a Millicell-ERS volt-ohmmeter by placing one electrode in the apical compartment (basket) and the other in the basolateral compartment (well). A TEER measurement of >300Ω is used as a baseline to represent a polarized monolayer. Cells were exposed to IC_{50} values of the inhibitors (either Verapamil or AR-C155858) in replicates of three for acute durations of 6, 12 and 24 hours and for a chronic duration of 7 days. Treatment was done in the apical compartment for Caco-2 cells as exposure is in the lumen and in the basolateral compartment for BME-UV cells as exposure is in the systemic circulation. TEER values and Lucifer Yellow (LY) rejection rates were measured at each time point on three separate occasions.

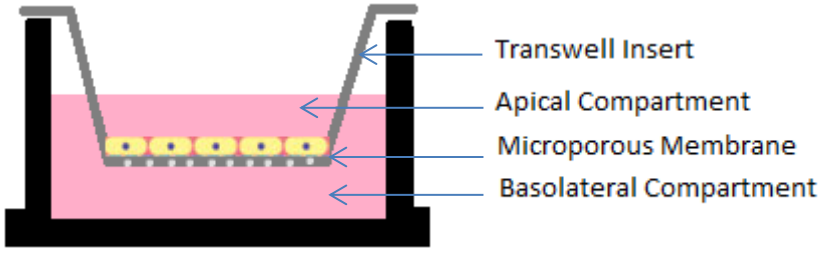

Figure 3.1: A schematic representation of the Transwell-based approach for *in vitro* barrier integrity assessment. A transwell insert with a microporous membrane (representing the apical compartment) rests in a well (representing the basolateral compartment). Cells are seeded in the apical compartment and the porous membrane allows the cells to interact with media on either side. Cells are cultured for a determined amount of time allowing a polarized monolayer to form.

3.4.1 Lucifer Yellow Rejection Rates

LY is routinely used to assess barrier integrity as it solely transverses the membrane by the paracellular route. Therefore, it is used as a measurement of barrier 'tightness'. An intact polarized barrier will reject ~99% of the LY. To make the LY solution, one mg of LY was dissolved in Hank`s Balanced Salt Solution (HBSS) with 2% HEPES 4-(2-hydroxyethyl)-1-piperazineethanesulfonic acid) added and stored at 4°C in an opaque tube. Media was carefully

removed in the apical compartment (basket of transwell) using suction as to not disrupt the monolayer of cells and washed twice with HBSS and HEPES solution and then 200 µL of Lucifer Yellow suspension was added. Media was removed from the basolateral compartment and replaced with HBSS and HEPES solution. The plate was incubated for 2 hours in 37°C at 5% CO_2. The transwell inserts were removed and the fluorescence of the basolateral compartment was read at 485/535 nm.

3.5 Acute and Chronic Effects of Inhibitor Exposure on Expression of Transporters

3.5.1 Total RNA Extraction

Following acute and chronic exposure to the inhibitors and measurement of LY rejection rates, cells were washed twice with HBSS with HEPES to remove any remaining LY. Two hundred µL of Trizol was added and was left to sit for 1 min to allow cell lysis and then the sample was collected and stored at -80°C. Total RNA was extracted using RNeasy Midi Kits according to manufacturer's instructions. Frozen cell pellets were thawed for 20 minutes at room temperature on counter sprayed with RNAseZAP. Cell lysate was then homogenized with 350 µL of buffer RLT containing β-ME and added to 1 volume of 70% ethanol to precipitate the nucleic acids. The cell lysate was then applied to the Midi column and a series of buffers were added to remove the cellular contaminants according to the manufacturer's instructions. The purified RNA was isolated from the column using RNase-free water (30 µL). The concentration and purity of isolated total RNA was determined using a Nanoview UV spectrophotomer (GE Healthcare Life Sciences, Quebec, Canada). Total RNA was quantified by measuring the absorbance of a diluted RNA (RNA:RNase-free water) at 260 nm according to the following formula:

$$\text{Concentration of RNA} = 40\ \mu g/mL \times A_{260} \times \text{Dilution factor}$$

RNA purity was assessed by measuring absorbance ratio (A_{260} / A_{280}) of a diluted sample of RNA (RNA:10 mM TrisCl (pH-7.5)). Pure RNA has a ratio between 1.9-2.1. Al1 samples used for qPCR were of high purity. Total RNA was stored at -80°C until analysis.

3.5.2 Primer Design

Gene sequences for OCTN1, OCTN2, MCT1, MCT2, and GADPH were obtained from the National Center for Biotechnology Information Gene Bank (NCBI) and specific primers were designed using Integrated DNA Technologies (https://www.idtdna.com/Primerquest/Home/Index).

Table 3.2: Primer sequences and annealing temperatures of selected transporters of interested designed using Integrated DNA Technologies.

Target Gene	Primer Sequence (5'-3')	Annealing Temperature (°C)
hOCTN1	F: GACAGGTTTGGCAGGAAGAA	55.2
	R: CATGCCCACGATGACAAATAAC	54.5
hOCTN2	F: GGGAGGTAGCATTTCCAATAA	54.6
	R: CATCAGAGGCTCCCAAATCTAC	55.0
hMCT1	F: GCTAGCACCTTTATCCACTACC	55.0
	R: GGTCCAACAAGGTCCATCAA	55.0
hMCT2	F: ATGGTGTTGGCCTCCTTTAG	54.9
	R: CAATTATGGTTAAGGCGGGTTG	54.4
hGADPH	F: GGTGTGAACCATGAGAAGTATGA	54.5
	R: GAGTCCTTCCACGATACCAAA	55.1
bOCTN1	F: CCCTGAAGCAGCAGAAAGT	55.2
	R: CCACTGAGGTCAACATCCATAG	54.9
bOCTN2	F: TCTTGGCAAGTCAGTTCGTATTA	54.0
	R: CGCCAGTCTCTGATGAAGTAAG	55.0
bMCT1	F: TGTGGGACTGAAGGGTAAATG	54.6
	R: CCTGGTATGATTCCCACAGAAA	54.5
bMCT2	F: AGAAACGACCTGTAGCGAATG	54.9
	R: GCTTCCCTTCCAACCATAAGT	54.9
bGAPDH	F: TGAGATCAAGAAGGTGAA	54.4
	R: GCATCGAAGGTAGAAGAGTGA	54.8

3.5.3 Optimization of Primers

Primer optimization was done using a SYBR Green RT-PCR reagent kit and an Applied Biosystems Real-Time PCR System (Foster City, California, USA). Primers were reconstituted to 100 µmol/L and then diluted to 5 µmol/L using UltraPure Distilled Water. Seven µL of SYBR Green, 2 µL of the respective forward and reverse primer, and 2 µL of 2 ng RNA (human or bovine) was added in a 96 well plate and spun down. Initial activation step (1 cycle at 95°C for 15 min) was followed by a three step thermal cycling (40 cycles; denaturing at 95°C for 15s, annealing at 60°C for 30s, and extension at 60°C for 30s). Finally, a melt curve analysis from 65°C to 95°C at 0.5°C/s was performed. Only primers that bound to one product and had a C_T value less than 25 were chosen and used for analysis.

3.5.4 cDNA Synthesis

cDNA was synthesized using the SuperScript VILO cDNA Synthesis Kit and a MyCycler Thermal Cycler System (Foster City, California, USA). Due to low RNA extraction yields (average of 50 ng/µL), 14 µL of RNA was added to 4 µL of VILO Reaction Mix and 2 µL of SuperScript Enzyme Mix. This kit allows for a dilution of 20x when RNA amounts exceeded 100 ng and this step was neglected due to low RNA yields. Contents were mixed and then incubated at 25°C for 10 minutes and then incubated at 42°C for 60 minutes. The reaction was terminated at 85°C for 5 minutes and the cDNA was stored at -20°C.

3.5.5 Quantitative Reverse Transcription-Polymerase Chain Reaction (qPCR)

The relative expression of mammary and intestinal monocarboxylate and L-carnitine transporters was determined using qPCR. One step qPCR reactions were performed using a SYBR Green RT-PCR reagent kit and an Applied Biosystems Real-Time PCR System (Foster City, California, USA). A 20 µL reaction mixture of 2x concentrated Power SYBR Green master mix, an optimized concentration of cDNA, gene specific qPCR primers, and nuclease free water was prepared for each cDNA sample and primer combination. Reactions were conducted in triplicate with an optimized 13 µL reaction volume per well. The reactions were quantified following determination of the threshold cycle (C_T; the amplification cycle when PCR products

are first detected above baseline fluorescence) and fluorescence was measured from the intercalation of SYBR green dye into the double stranded product after the primer elongation phase. A non-template negative control was incorporated into all analysis runs. PCR products were analyzed using comparative C_T or $2^{-\Delta\Delta C}{}_T$ method. Initial activation step (1 cycle at 95°C for 15 min) was followed by a three step thermal cycling (40 cycles; denaturing at 95°C for 15s, annealing at 60°C for 30s, and extension at 60°C for 30s). Finally, a melt curve analysis from 65°C to 95°C at 0.5°C/s was performed.

3.6 CellTiter-Glo® Luminescent Cell Viability

Cells were seeded at a density of 50,000 cells/100 µL per well in luminescent 96 well plates and incubated at 37°C with 5% CO_2 for 24 hours to allow for cell attachment. Control wells were also prepared containing media without cells to obtain a value for background luminescence. Following the 24 hour incubation the cells were treated with either Verapamil or AR-C155858 at their respectable IC_{50} concentrations for 6 hours. After treatment, the cells were allowed to equilibrate to room temperature for 30 minutes. During this time, the CellTiter-Glo Buffer and Substrate were thawed and allowed to equilibrate to room temperature prior to use. Ten mL of Buffer was added to Substrate to reconstitute the lyophilized enzyme/substrate mixture forming the CellTiter-Glo Reagent. The Reagent was mixed by gently inverting. Reagent was added to the wells within 1 minute of preparation. A 100 µL volume of Reagent was added to each well and the contents were mixed for 2 minutes on an orbital shaker to induce cell lysis. The plate was allowed to incubate at room temperature to stabilize the signal and then the luminescence was recorded. Assay was performed in triplicate on three separate occasions.

3.7 pH-Xtra Glycolysis Assay

Cells were seeded at a density of 50,000 cells/100 µL per well in 96 well plates and incubated at 37°C with 5% CO_2 for 24 hours to allow them to attach. Control wells were also prepared containing media without cells to obtain a value for background signal. Respiration Buffer tablet was reconstituted in 50 mL of water and the pH was adjusted to 7.4 and filter sterilized using a 0.22 µm filter. One mL of Respiration Buffer was added to the pH-Xtra vial and the contents were reconstituted by gently inverting. Prior to commencing the assay, all media and stock solutions used were pre-warmed to 37°C prior to use and the plate was kept on a block

heater during plate preparation. Spent medium was removed for the wells and washed twice using 100 µL of Respiration Buffer. After the second wash, 150 µL of fresh Respiration Buffer was added. Ten µL of the reconstituted pH-Xtra reagent was added to each well, except those used as blank controls. Ten µL of either inhibitor was added at the concentration of their respective IC_{50} value. Ten µL of 10 µM of Antimycin (Complex III Inhibitor) was used as a negative control. The plate was read kinetically for 120 minutes on a fluorescence plate reader at 320/620nm. Assay was performed in triplicate on three separate occasions.

3.8 MitoXpress Xtra Oxygen Consumption Assay

Cells were seeded at a density of 50,000 cells/100 µL per well in 96 well plates and incubated at 37°C with 5% CO_2 for 24 hours to allow them to attach. Control wells were also prepared containing media without cells to obtain a value for background signal. The contents of the MitoXpress Xtra vial was reconstituted in 1 mL of DMEM and gently inverted to mix. Prior to commencing the assay, all media and stock solutions used were pre-warmed to 37°C prior to use and the plate was kept on a block heater during plate preparation. Following the 24 hour incubation, spent culture media was removed and replaced with 150 µL of fresh media. Ten µL of the reconstituted MitoXpress reagent was added to each well, except those used as blank controls. Ten µL of either inhibitor was added at the concentration of their respective IC_{50} value. Ten µL of 10 µM of Antimycin (Complex III Inhibitor) was used as a negative control. The plate was read kinetically for 120 minutes on a fluorescence plate reader at 380/645nm. Assay was performed in triplicate on three separate occasions.

3.9 Statistical Analysis

Data was analyzed by one-way or two-way ANOVA followed by Tukey's multiple comparison test as appropriate. A P-value > 0.05 was taken to indicate a significant difference between the means of sets of data. All experiments were conducted in triplicate on three separate occasions with the data being expressed as mean ± standard deviation (SD).

4. RESULTS

4.1 Barrier Integrity – TEER measurements and LY Rejection Rates

To assess the integrity of the epithelial systems, cells were seeded in polyester membrane transwells in the apical compartment (inserts measure 24 mm in diameter and have a pore size of 0.4 µm) and allowed 3 weeks to form a polarized epithelium. Initial TEER measurements were obtained using a Millicell-ERS volt-ohmmeter and a TEER measurement of >300Ω is used as a baseline to represent a polarized monolayer. Cells were exposed to IC_{50} values of the inhibitors (either Verapamil or AR-C155858) in replicates of three for acute durations of 6, 12 and 24 hours and for a chronic duration of 7 days with TEER values and Lucifer Yellow (LY) rejection rates measured at each time point on three separate occasions. No significant variation for TEER values and LY rejection rates were found at any time point between the control and treated groups in either cell line.

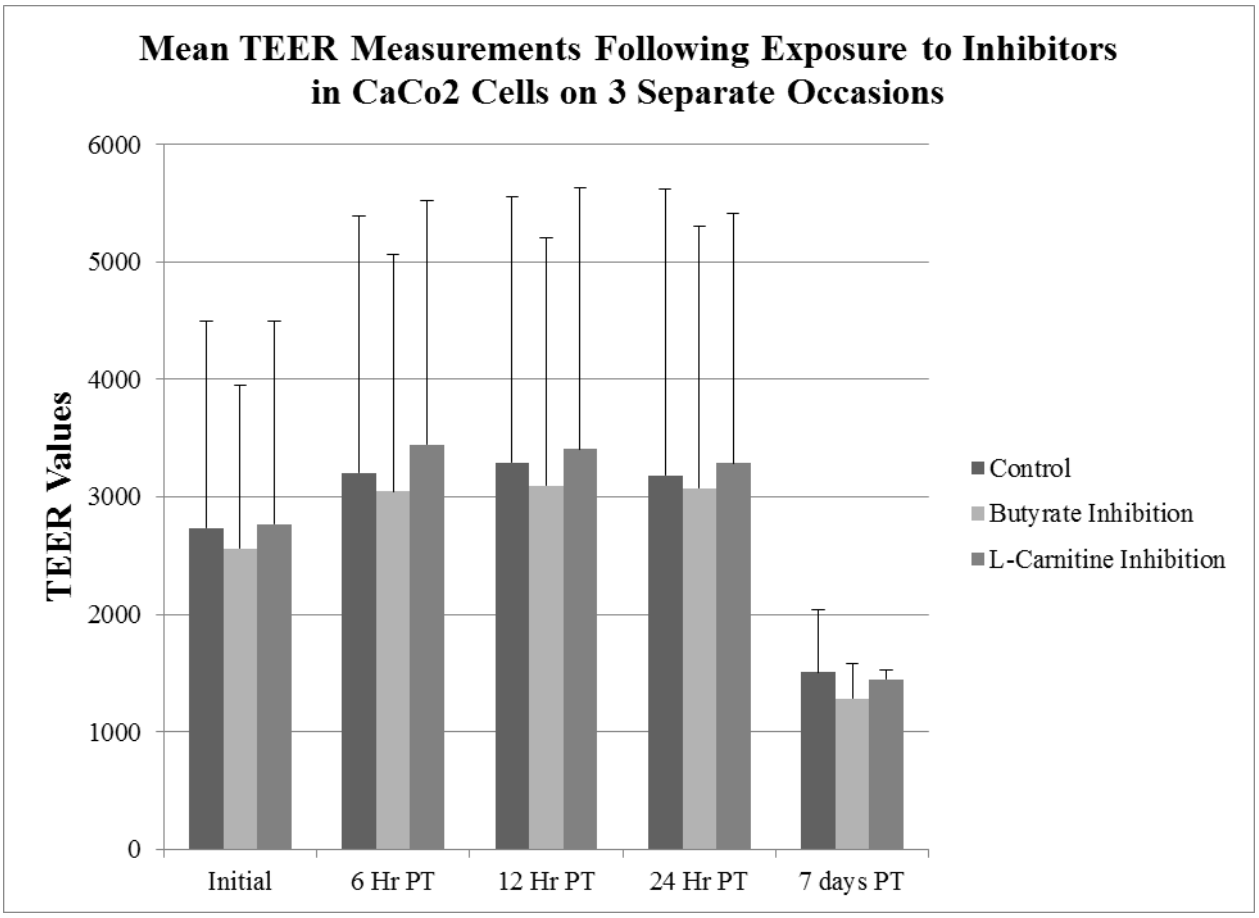

Figure 4.2: Mean ± SD of transepithelial electrical resistance (TEER) values in Caco2 cells at 5 different time points with and without treatment of butyrate or L-carnitine transporter inhibitors ran in replicates of three on three separate occasions. A TEER measurement of 300Ω is used as a threshold to represent a polarized monolayer has formed. Initial TEER values were taken prior to treatment and were taken again at 6, 12, 24 hr and 7 days post-treatment (PT). Means were compared using one-way ANOVA ($P < 0.05$) followed by Tukey's test to know the interaction between control and treatment groups. No significant difference was determined between control and treatment groups.

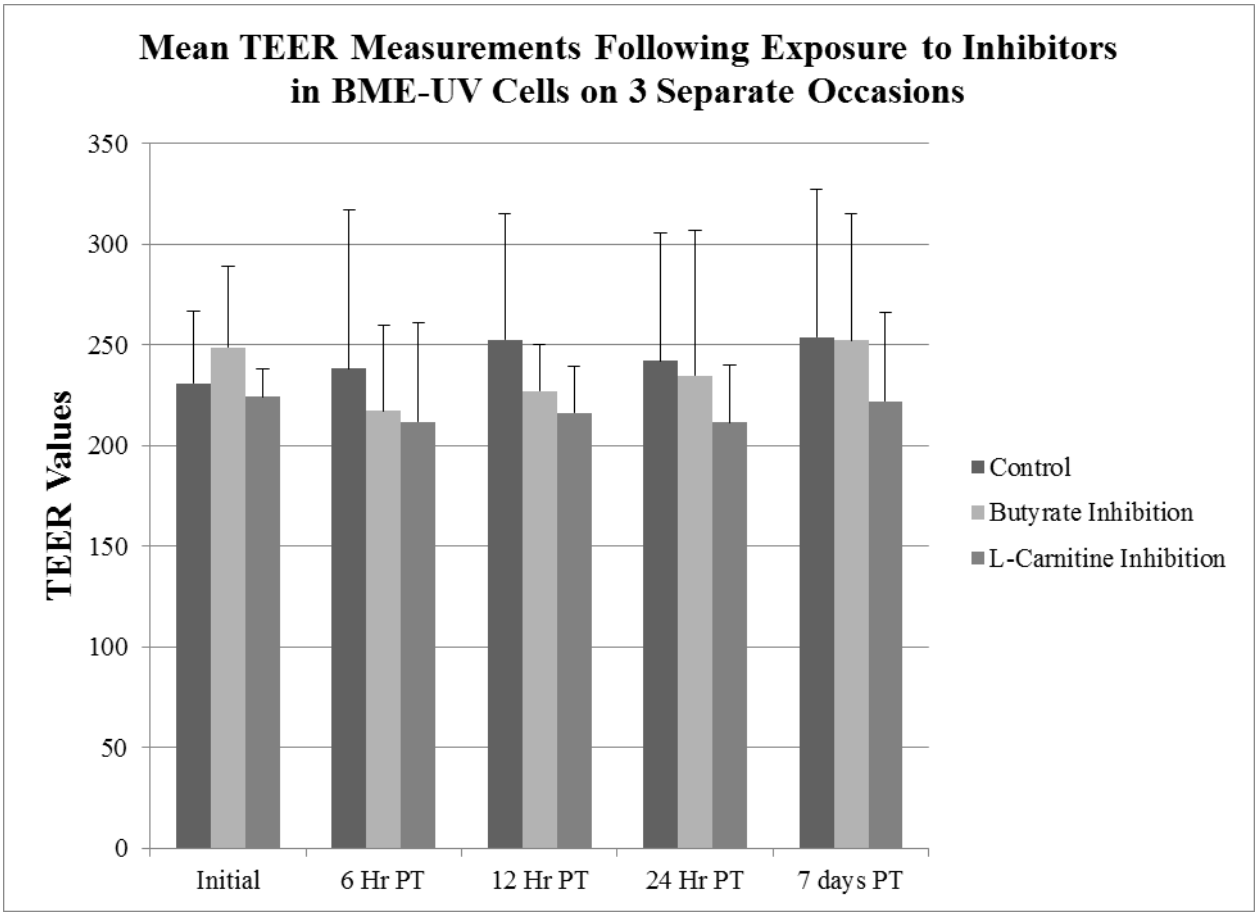

Figure 4.3: Mean ± SD of transepithelial electrical resistance (TEER) values of BME-UV cells at five different time points with and without treatment of butyrate or L-carnitine transporter inhibitors ran in replicates of three on three separate occasions. A TEER measurement of 300Ω is used as a threshold to represent a polarized monolayer has formed. Initial TEER values were taken prior to treatment and were taken again at 6, 12, 24 hr and 7 days post-treatment (PT).

Means were compared using one-way ANOVA ($P < 0.05$) followed by Tukey's test to know the interaction between control and treatment groups. No significant difference was determined between controls and treatment groups.

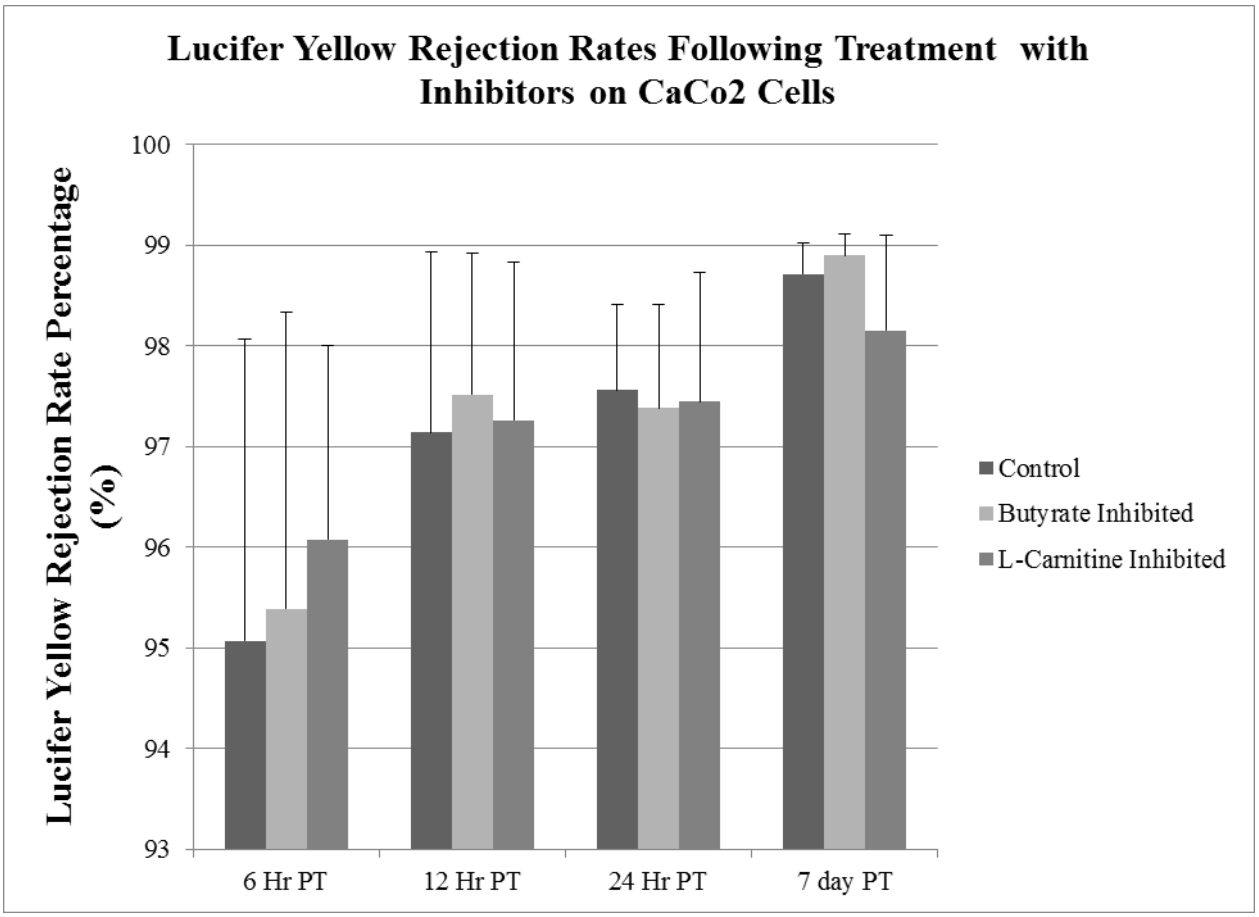

Figure 4.4: Mean ± SD of Lucifer Yellow (LY) Rejection Rate percentages of Caco-2 cells at 4 different time points with and without treatment of butyrate or L-carnitine transporter inhibitors ran in replicates of three on three separate occasions. A rejection rate of >95% is used as a threshold to represent an intact barrier has formed. LY rejection rates were measured following treatment for 6, 12, 24 hr and 7 days. Means were compared using one-way ANOVA ($P < 0.05$) followed by Tukey's test to know the interaction between control and treatment groups. No significant variation was determined between control and treatment groups.

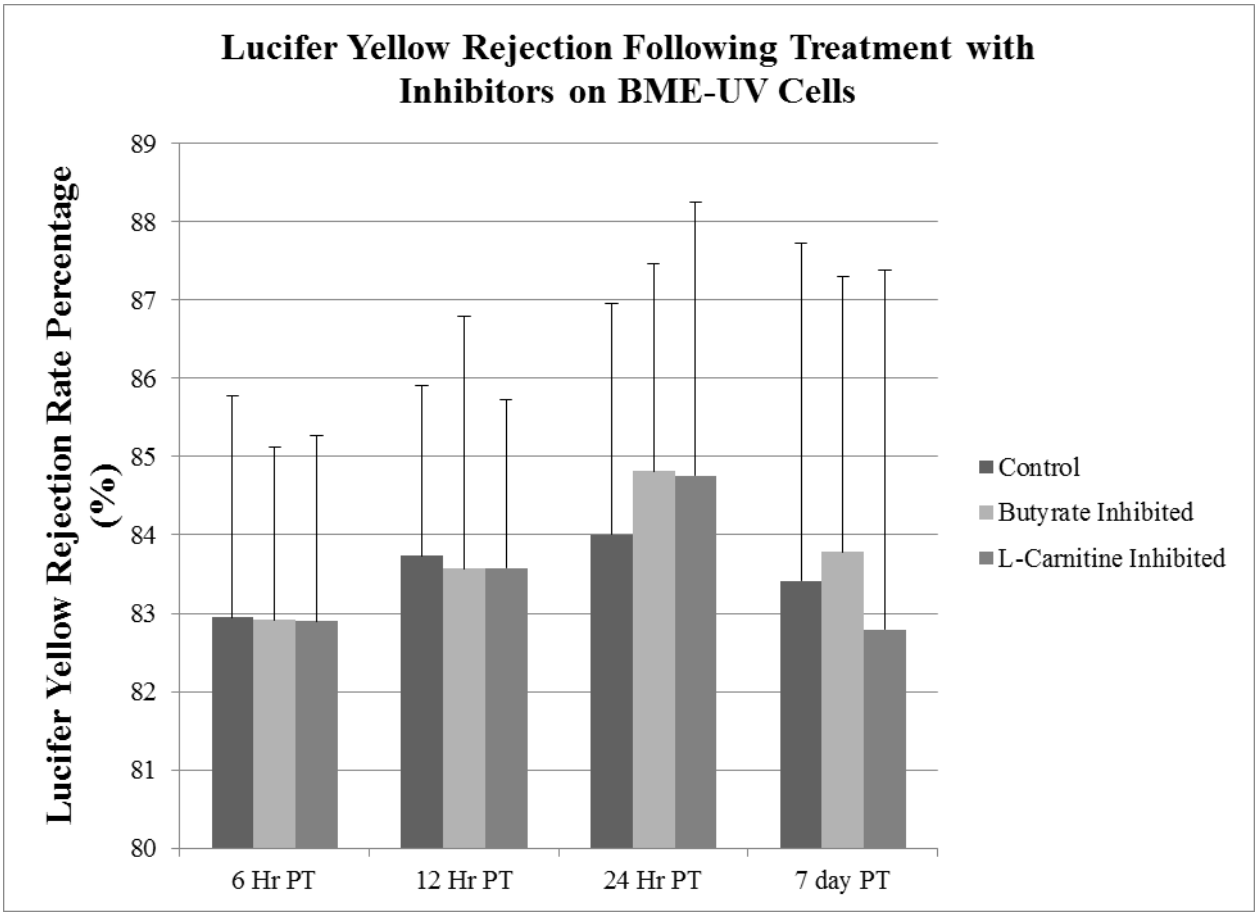

Figure 4.5: Mean ± SD of Lucifer Yellow (LY) Rejection Rate percentages of BME-UV cells at 4 different time points with and without treatment of butyrate or L-carnitine transporter inhibitors ran in replicates of three on three separate occasions. A rejection rate of >95% is used as a threshold to represent an intact barrier has formed. LY rejection rates were measured following treatment for 6, 12, 24 hr and 7 days. Means were compared using one-way ANOVA ($P < 0.05$) followed by Tukey's test to know the interaction between control and treatment groups. No significant variation was determined between controls and treatment groups.

4.2 Barrier Integrity – Transporter Expression

To assess the expression of key transporters involved in the transport of L-carnitine and butyrate following acute (6, 12, and 24 hours) and chronic (7 days) exposure to their respective drug inhibitors, RNA was extracted for qPCR analysis. A low RNA yield was noted and cDNA synthesis protocol was altered to compensate. qPCR reactions were ran with poor results. Only the housekeeping gene (GADPH) was observed in Caco-2 cells along with OCTN1 and OCTN2 in BME-UV cells, however, C_T values were too high to be quantified appropriately by the instrument.

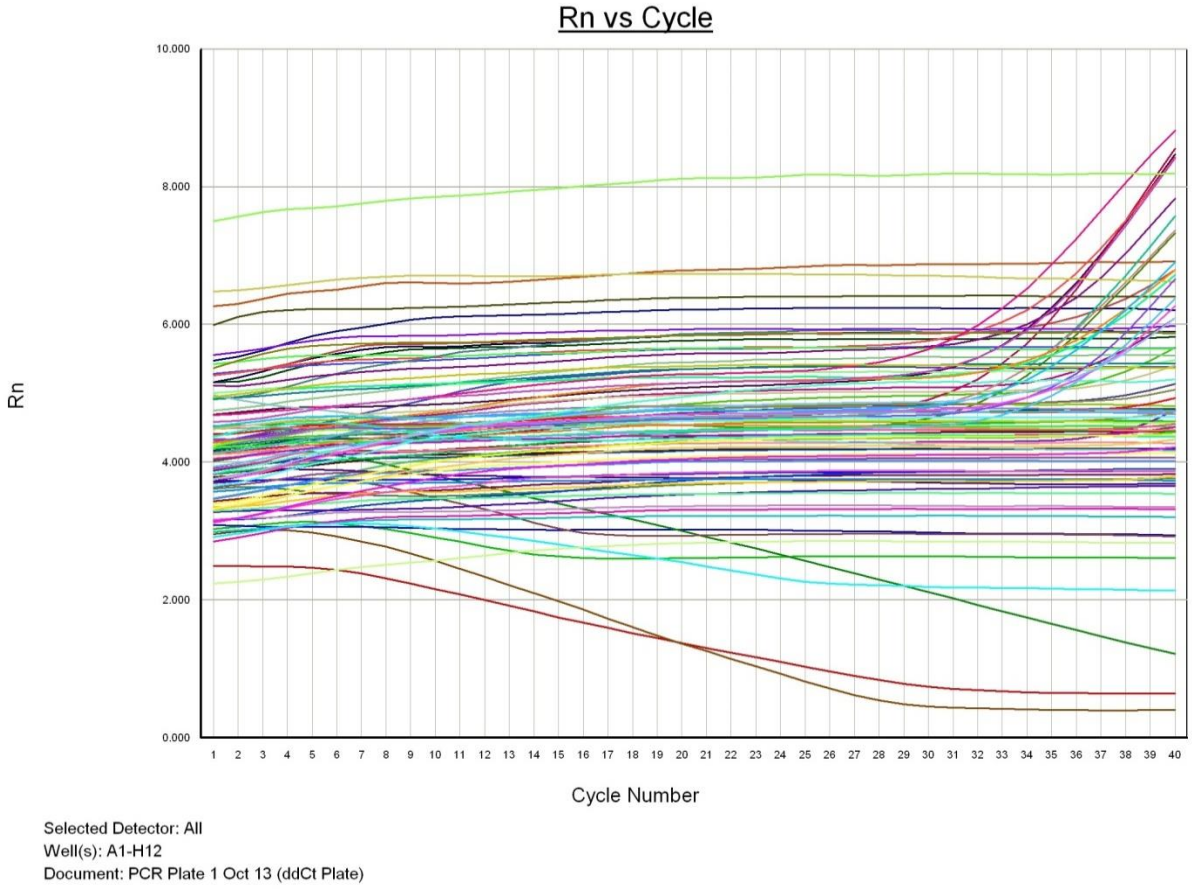

Figure 4.6: Real time RT-PCR readout of the association stage looking at an increase in fluorescence (from the intercalation of SYBR Green dye in amplifying DNA) with PCR cycle in Caco-2 cells. The transporters OCTN1, OCTN2, MCT1, MCT2 and the housekeeping gene, GADPH, were measured with each line representing the amplification of an individual

transporter. Only GADPH was amplified, but all C_T values were too high to be detected by the instrument, therefore, the expression could not be quantified.

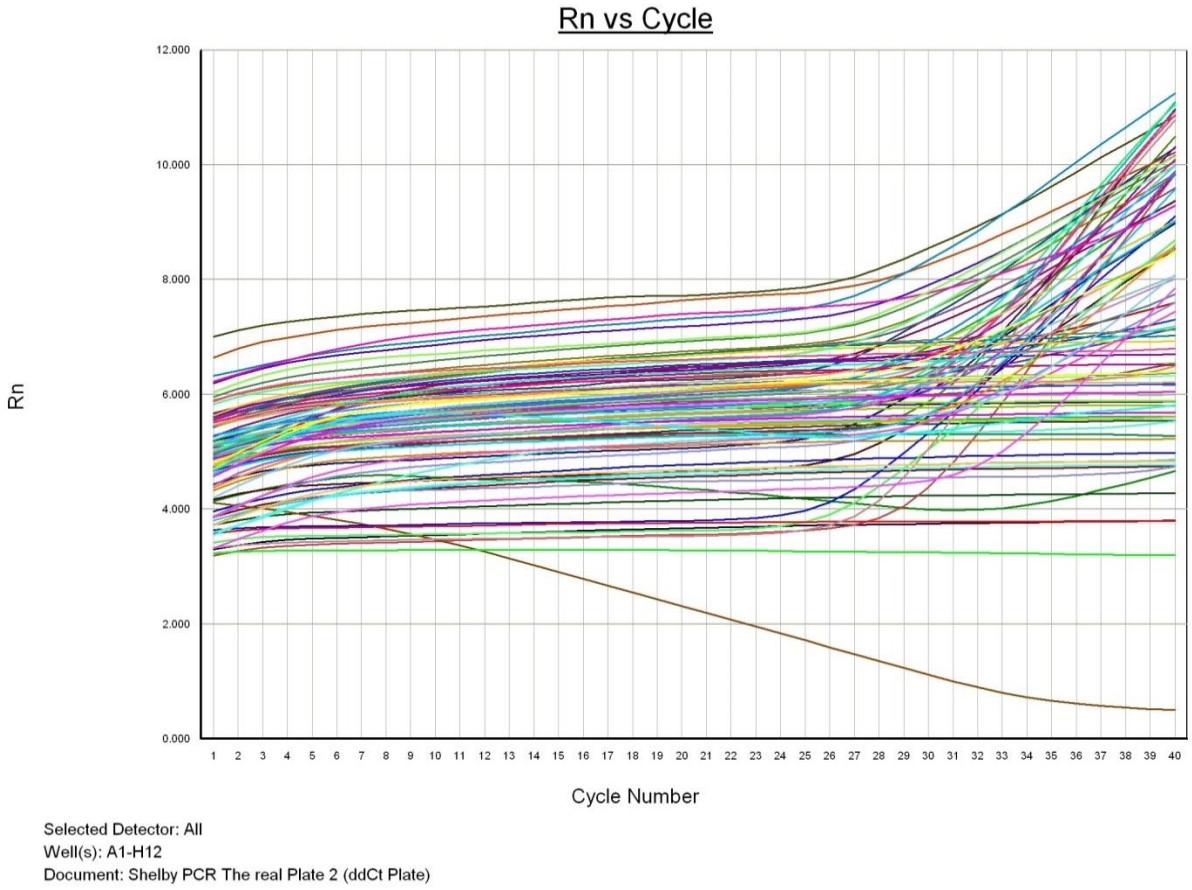

Figure 4.7: Real time RT-PCR readout of the association stage looking at an increase in fluorescence (from the intercalation of SYBR Green dye in amplifying DNA) with PCR cycle in BME-UV cells. The transporters OCTN1, OCTN2, MCT1, MCT2 and the housekeeping gene, GADPH, were measured with each line representing the amplification of an individual transporter. Only OCTN1, OCTN2 and GADPH were amplified, but all C_T values were too high to be detected by the instrument, therefore, the expression could not be quantified.

4.3 Cellular Homeostasis – ATP Synthesis

To assess ATP Synthesis, the CellTiter-Glo Luminescent Cell Viability Assay was used which is a method used to determine the number of viable cells based on the quantification of ATP present. A direct relationship exists between luminescence measured and the number of cells in culture which is directly proportional to the amount of ATP. No significant variation was found between the control groups and the treated groups in either cell lines.

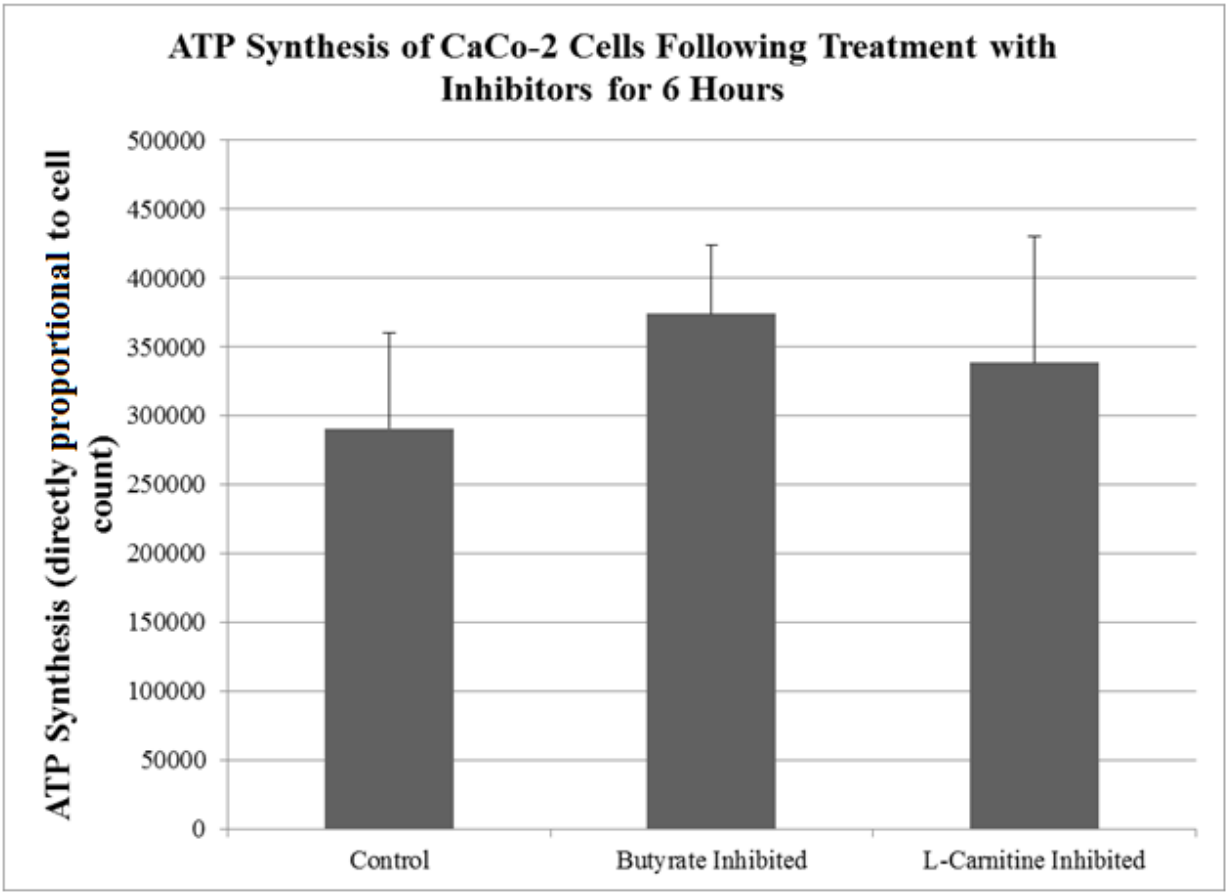

Figure 4.8: Values represent the mean ± SD of the ATP Synthesis by Caco-2 cells with and without treatment of butyrate or L-carnitine transporter inhibitors within 3 replicates on 3 separate occasions. A direct relationship exists between luminescence measured and number of cells in the culture which is directly proportional to ATP synthesis. Means were compared using one-way ANOVA ($P < 0.05$) followed by Tukey's test to know the interaction between control and treatment groups. No significant difference was determined between controls and treatment groups.

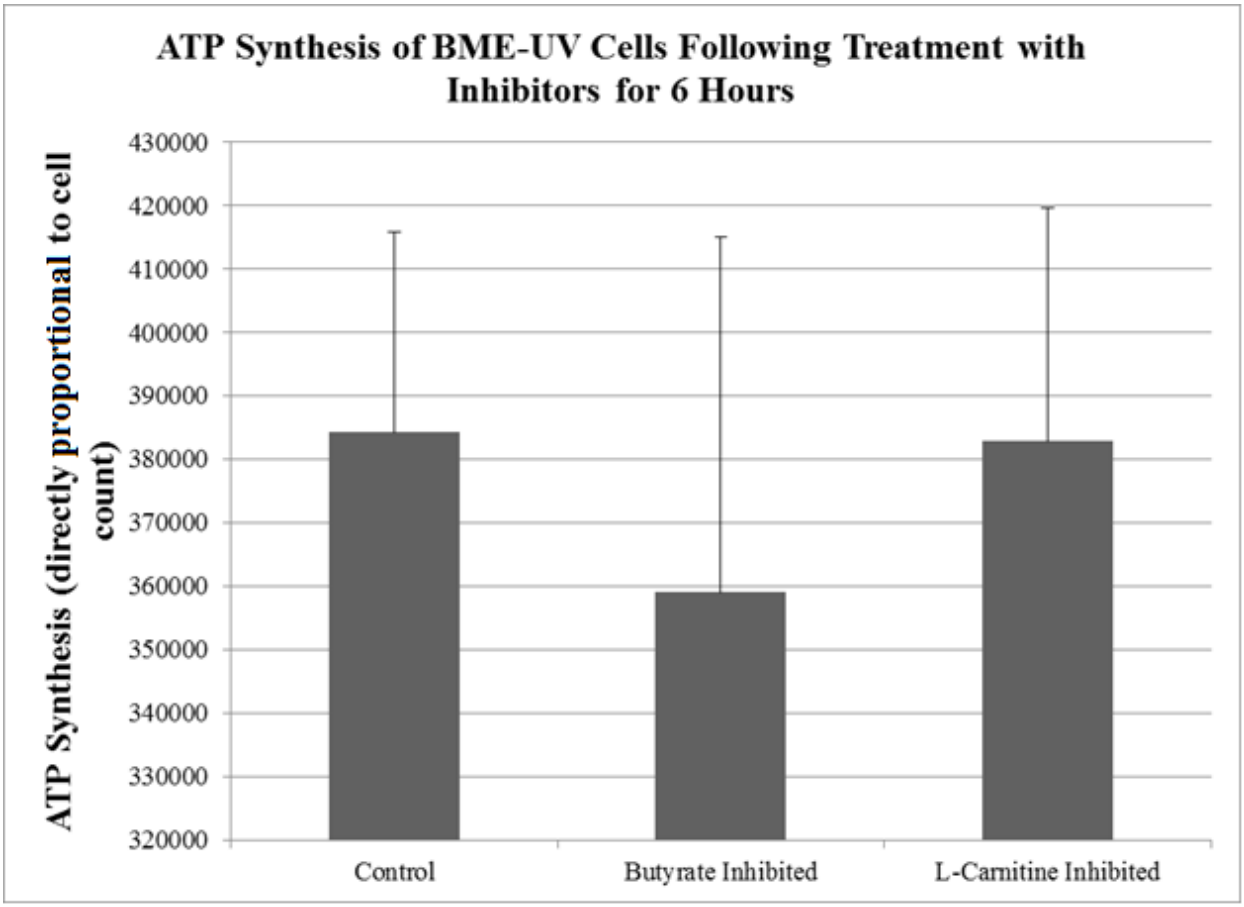

Figure 4.9: Values represent the mean ± SD of the ATP Synthesis by BME-UV cells with and without treatment of butyrate or L-carnitine transporter inhibitors within 3 replicates on 3 separate occasions. A direct relationship exists between luminescence measured and number of cells in the culture which is directly proportional to ATP synthesis. Means were compared using one-way ANOVA ($P < 0.05$) followed by Tukey's test to know the interaction between control and treatment groups. No significant variation was determined between controls and treatment groups.

4.4 Cellular Homeostasis – Glycolysis

To assess glycolytic flux, the pH-Xtra Glycolysis Assay was used which measures the real-time, kinetic analysis of extracellular acidification (ECA) rates. Lactate production is the main contributor to ECA; therefore, the measurement of ECA is a convenient measurement of cellular glycolytic flux. Cells were seeded at a density of 50,000 cells/well (for both cell lines) and allowed to attach before being treated for 6 hours with the respective inhibitor. Optional controls were noted in the protocol, and three out of the four were employed. Blank controls were free from the addition of pH-Xtra Reagent and signal controls included wells left absent from the addition of cells. Antimycin A was used as a positive control as it blocks cellular respiration resulting in an increase in lactate formation. Upward trends were noted in both the Caco-2 cells and the BME-UV cells as well as wells treated with both inhibitors over the 120 minute period.

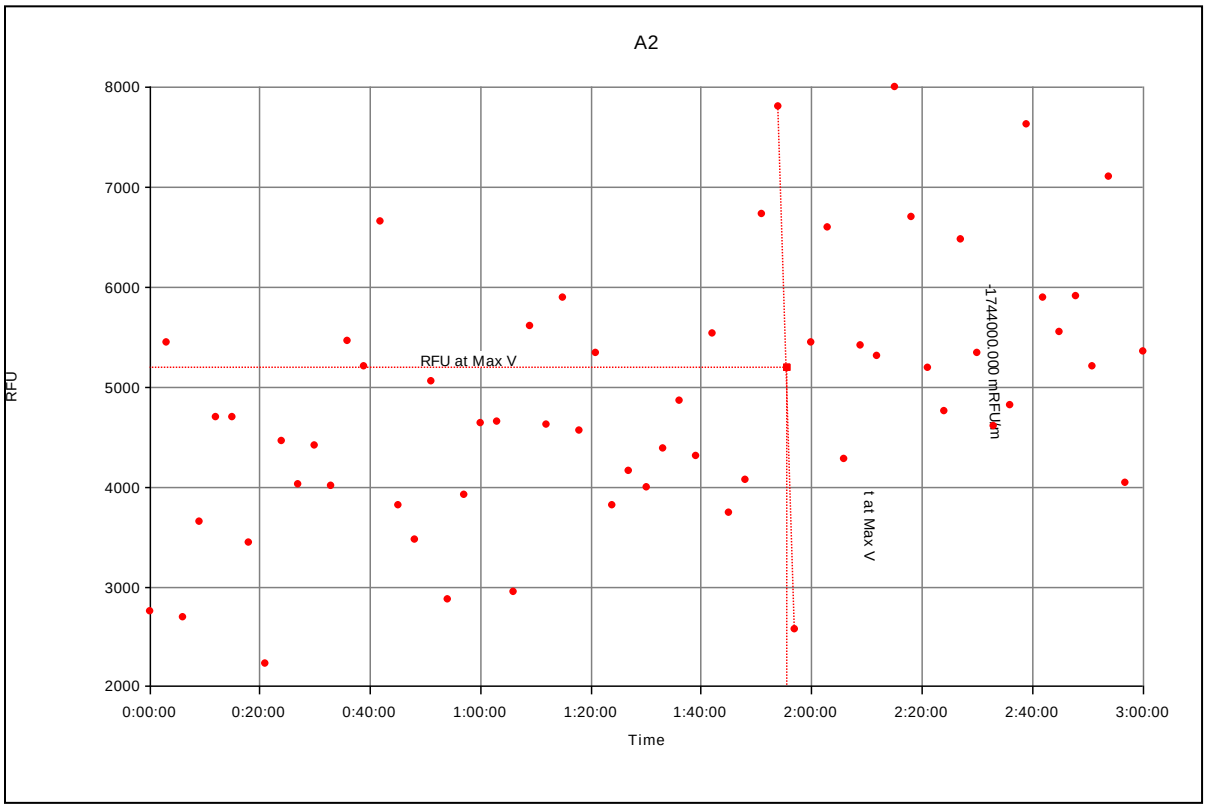

Figure 4.10: Representative graph of pH-Xtra Glycolysis Assay of Caco-2 cells treated with AR-C155858. This is a plot of relative fluorescence units (RFU) as a function of time where increases in RFU indicate increasing extracellular acidification (ECA). The slope of the graph is equivalent to the ECA measurement. An upward trend was noted in all wells treated with the

IC_{50} of AR-C155858 (butyrate inhibitor) and Verapamil (L-carnitine inhibitor) in both the Caco-2 cell line as well as the BME-UV cell line.

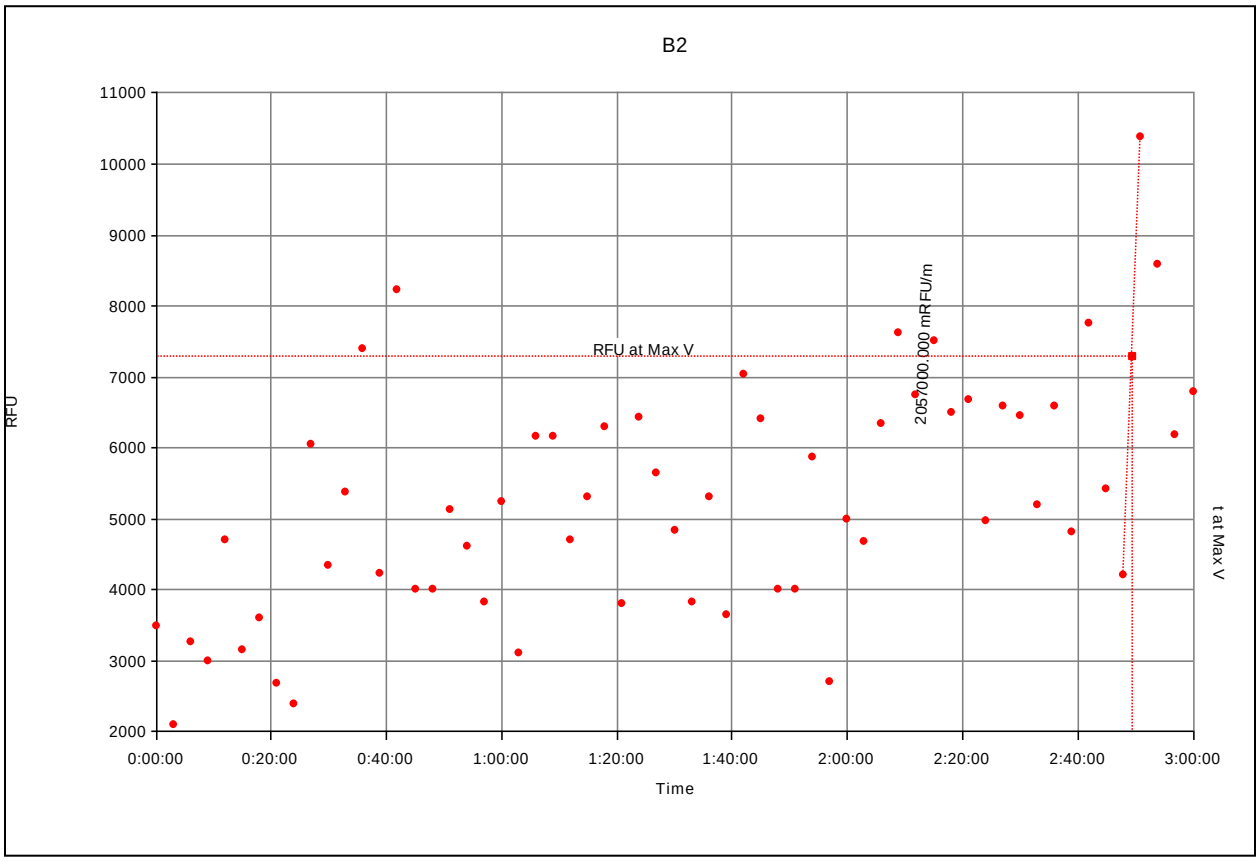

Figure 4.11: Representative graph of pH-Xtra Glycolysis Assay of Caco-2 cells treated with the positive control, Antimycin A. Antimycin A blocks cellular respiration resulting in an increase in lactate formation, which further results in an increase in extracellular acidification (ECA). This is a plot of relative fluorescence units (RFU) as a function of time where increases in RFU indicate increasing ECA. The slope of the graph is equivalent to the ECA measurement. An upward trend was noted in all wells treated with Antimycin A.

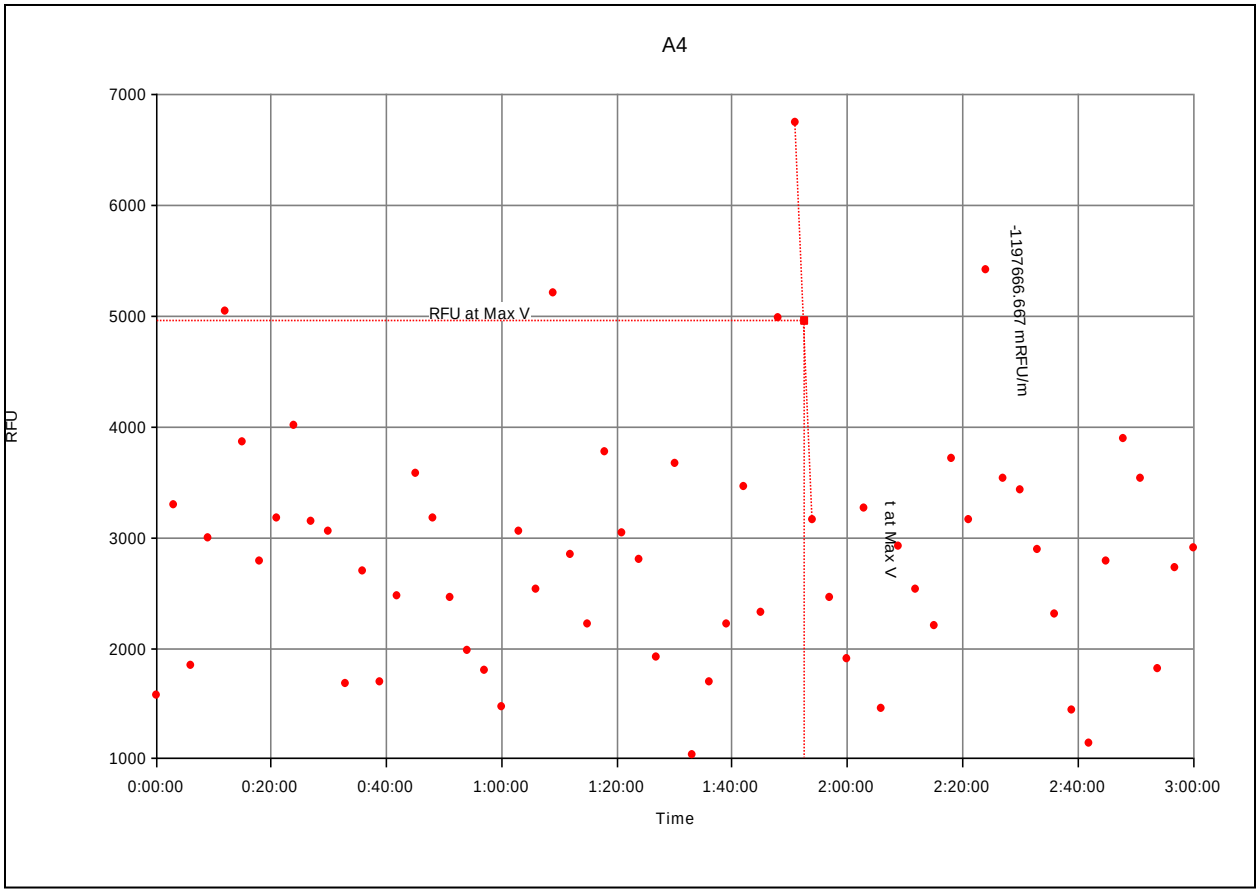

Figure 4.12: Representative graph of pH-Xtra Glycolysis Assay of wells of Caco-2 cells untreated with transporter inhibitor. This is a plot of relative fluorescence units (RFU) as a function of time where increases in RFU indicate increasing extracellular acidification (ECA). The slope of the graph is equivalent to the ECA measurement.

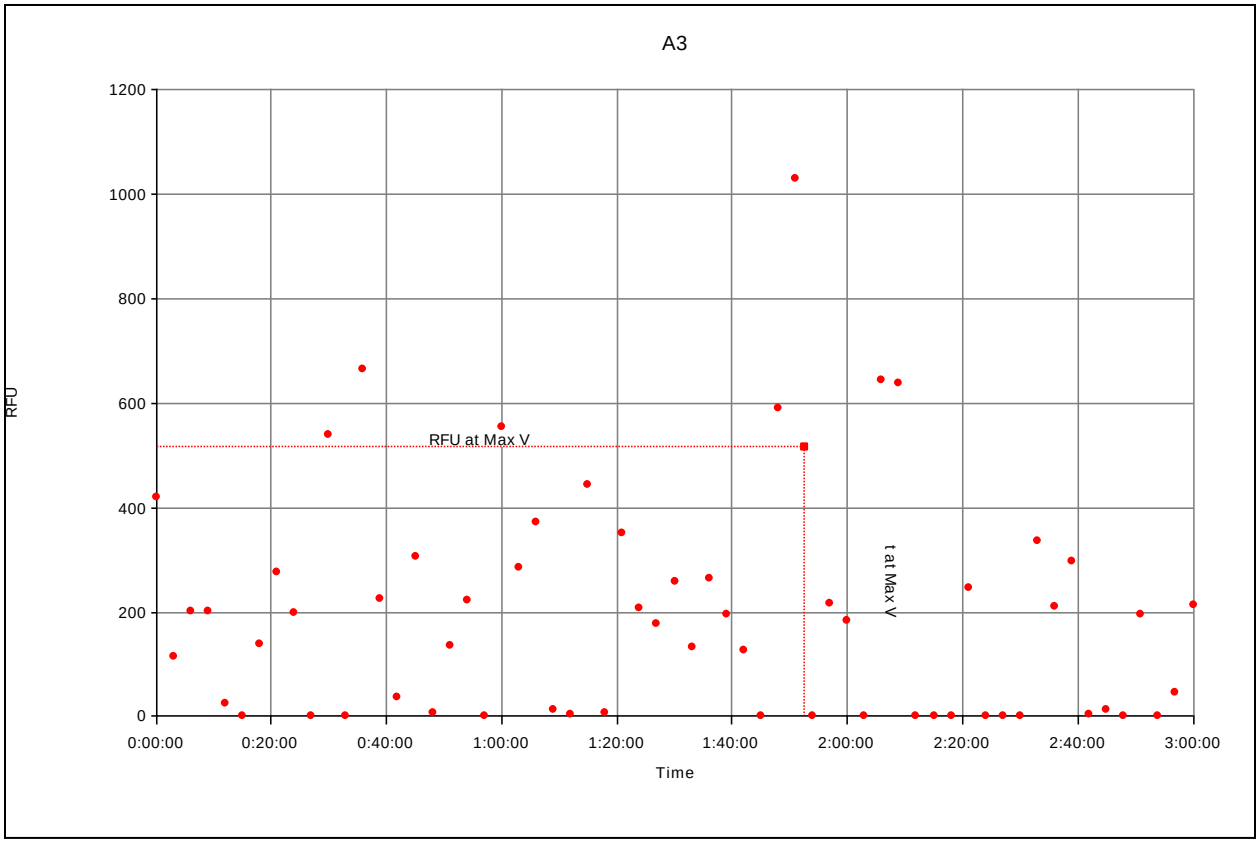

Figure 4.13: Representative graph of pH-Xtra Glycolysis Assay of the Blank Control (no pH Xtra added) in Caco-2 cells. This is a plot of relative fluorescence units (RFU) as a function of time where increases in RFU indicate increasing extracellular acidification (ECA). The slope of the graph is equivalent to the ECA measurement.

4.5 Cellular Homeostasis – Oxygen Consumption

To assess oxygen consumption rates the MitoXpress Xtra Oxygen Consumption Assay was used which measures the real-time, kinetic analysis of cellular respiration. The slope of the graph is representative of the Oxygen Consumption Rate (OCR). Cells were seeded at a density of 50,000 cells/well (for both cell lines) and allowed to attach before being treated for 6 hours with the respective inhibitor. Optional controls were noted in the protocol, and three out of the four were employed. Blank controls were free from the addition of MitoXpress Reagent and signal controls included wells left absent from the addition of cells. Antimycin A was used as a negative control as it is a Complex III inhibitor.

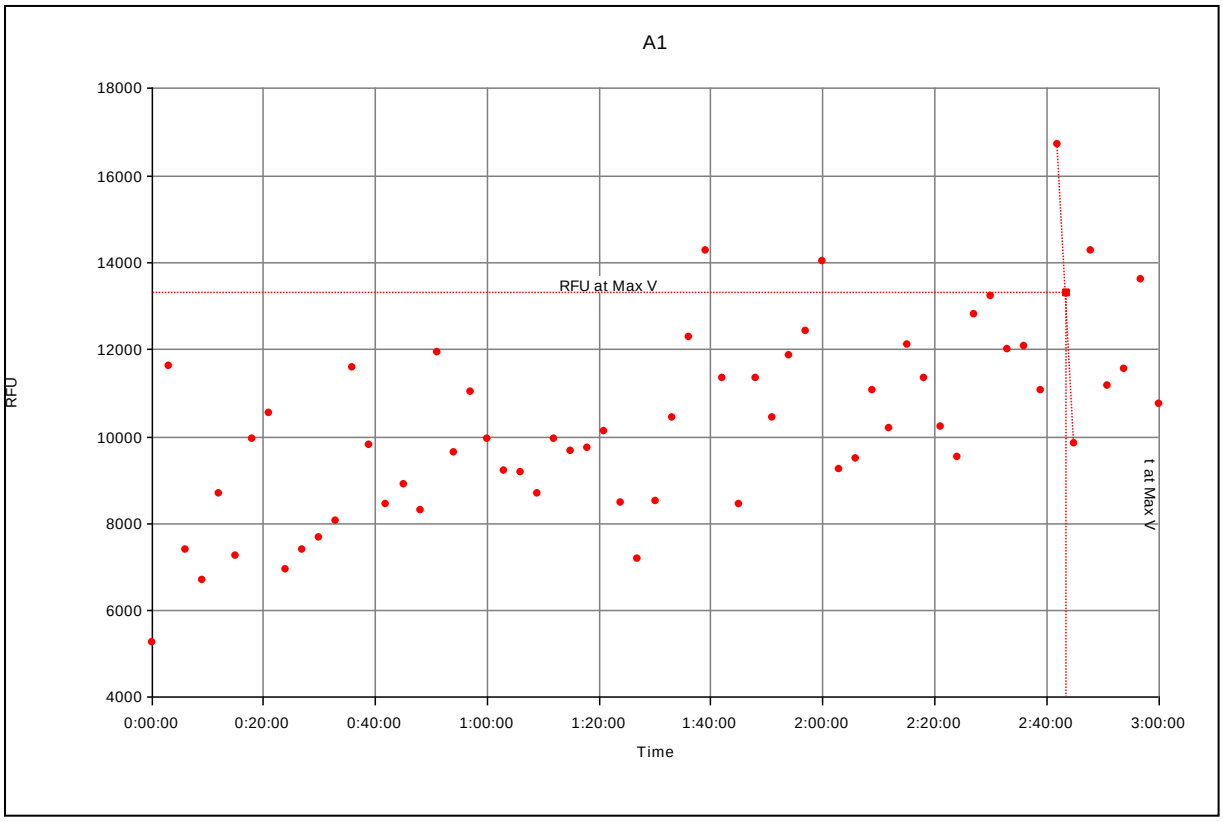

Figure 4.14: Representative graph of MitoXpress Xtra Oxygen Consumption Assay of Caco-2 cells treated with Verapamil. This is a plot of relative fluorescence units (RFU) as a function of time where increases in RFU indicate increasing oxygen consumption rate (OCR). The slope of the graph is equivalent to the OCR. An upward trend was noted in all wells treated with the IC_{50} of AR-C155858 (butyrate inhibitor) and Verapamil (L-carnitine inhibitor) in both the Caco-2 cell line as well as the BME-UV cell line.

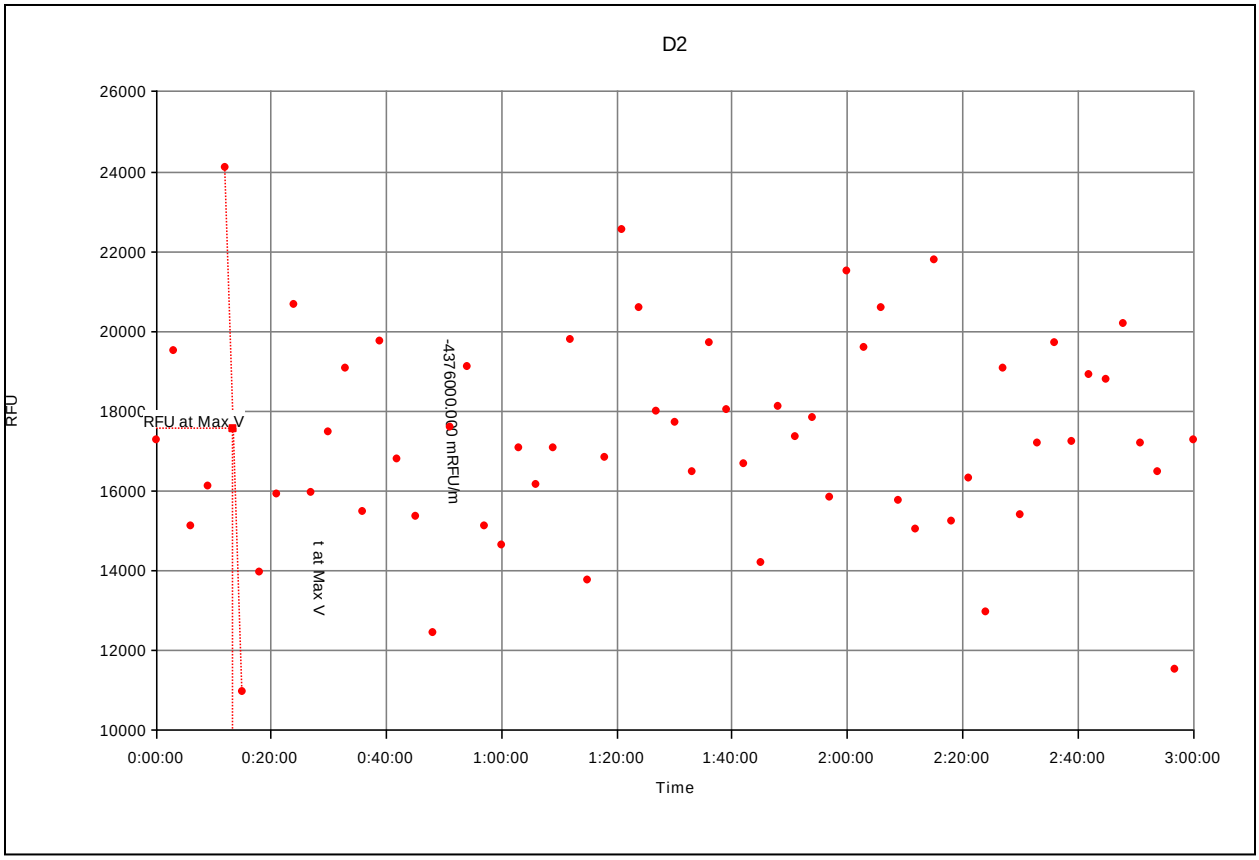

Figure 4.15: Representative graph of MitoXpress Xtra Oxygen Consumption Assay of Caco-2 cells treated with the negative control, Antimycin A. This is a plot of relative fluorescence units (RFU) as a function of time where increases in RFU indicate increasing oxygen consumption rate (OCR). The slope of the graph is equivalent to the OCR.

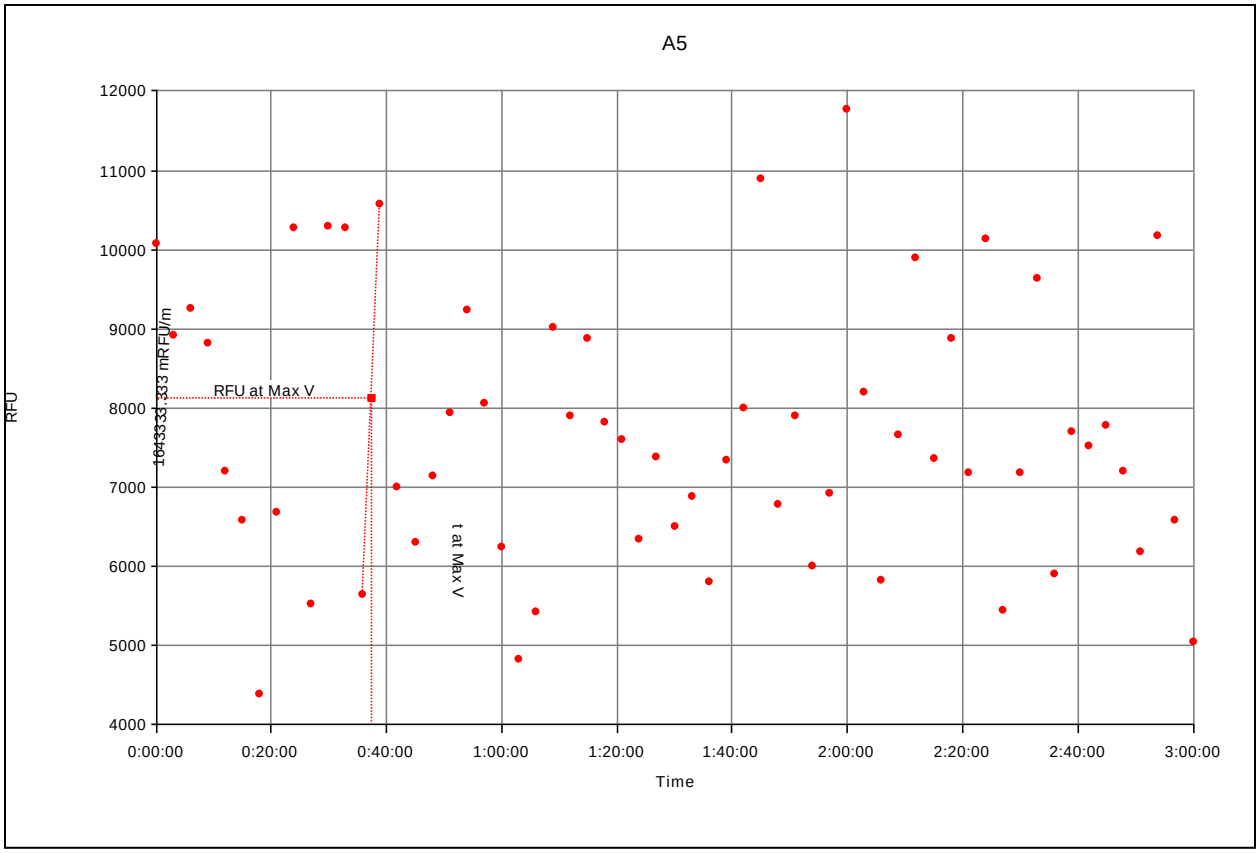

Figure 4.16: Representative graph of MitoXpress Oxygen Consumption Assay of wells of Caco-2 cells untreated with transporter inhibitor. This is a plot of relative fluorescence units (RFU) as a function of time where increases in RFU indicate increasing oxygen consumption rate (OCR). The slope of the graph is equivalent to the OCR.

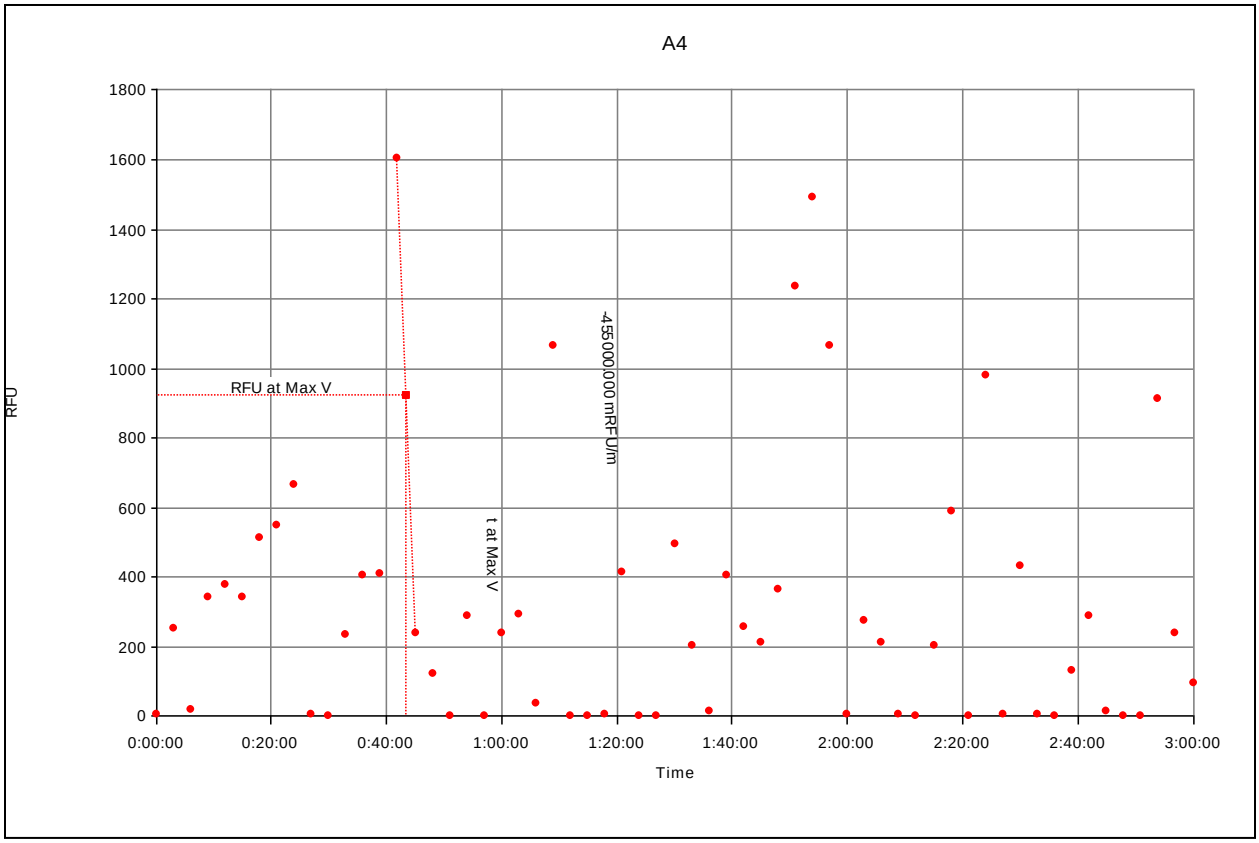

Figure 4.17: Representative graph of MitoXpress Oxygen Consumption Assay of the Blank Control (no MitoXpress added) in Caco-2 cells. This is a plot of relative fluorescence units (RFU) as a function of time where increases in RFU indicate increasing oxygen consumption rate (OCR). The slope of the graph is equivalent to the OCR.

5. DISCUSSION

The transporters primarily responsible for transporting the essential nutrients (L-carnitine and butyrate) involved in energy metabolism, OCTN2 and MCT1, have a wide substrate specificity setting up the potential for drug-nutrient transporter interactions. Pharmacological inhibition of nutrient transport across the lactating mammary and neonatal intestinal epithelial barrier can directly and indirectly affect growth and maturation of the developing neonate. This can be the result of direct competitive inhibition of these key nutrient transporters. Such inhibition might cause a reduction in the flux of L-carnitine and butyrate across the barriers decreasing their availability to the developing neonate. Due to the essentiality of these nutrients on energy metabolism, pharmacological inhibition of these transporters may also have indirect effects through an ability to disrupt barrier integrity due to a loss of cellular homeostasis. In particular, loss of intestinal barrier integrity may have important adverse effects on the neonate including sepsis and malnutrition.

Drug-nutrient interactions have been well documented in many systems including the GI tract, kidney and liver while some areas, including the mammary gland, have received limited attention (59). Drug induced inhibition of nutrient transporters, such as MCT1 and OCTN2, is increasingly being recognized as an important toxicological mechanism due to the possibility for severe consequences related to such interactions (9, 57). Although limited research is available, a few studies in the literature indicate the possibility of pharmacological inhibition of nutrient transporters at the mammary epithelium. Previous work in the Alcorn lab has shown pharmacological inhibition of transporters at the mammary gland impacts milk concentrations of L-carnitine, thus affecting availability of this nutrient to the neonate (9, 88). Changes in transporter expression has been shown to vary, following five key patterns, depending on the duration of lactation corresponding with the needs of the developing neonate at that time (9, 10). The varying expression of OCTNs allow for a greater drug-nutrient interaction involving L-carnitine when OCTN expression levels are high, resulting in significant differences in milk-serum ratios of L-carnitine as well as different consequences of a drug-nutrient transporter interaction (9). When mammary epithelial monolayers were challenged with inflammatory stimulus, an increase in maximal activity (V_{max}) of L-carnitine transport without an effect on the affinity (K_m) was noted. This corresponded to changes in cellular energy levels and oxygen

consumption rates (Uma Manthena MSc Thesis). Further, when the transporters were challenged with D-lactate, an inhibitor of transport by MCTs, a 75% reduction in cellular respiration was noted (88). As an extension to this, the premise of my work originally set out to focus on the impacts of pharmacological inhibition of nutrient transporters on the flux of essential nutrients as a proof of concept of the potential adverse effects related to nursing neonate when the lactating mother requires medication.

Many interactions have been documented in the intestinal epithelium involving MCT1, which is of concern as this is the primary transporter of butyrate, the SCFA that represents 70% of the energy source for colonic cells (59, 64, 65, 67). The mammary gland primarily relies on glycolysis to supply its energy and, therefore, these two epithelial systems have differing energy sources (24). Due to the different energy requirement of the two systems, we looked at the effects transport inhibition of those nutrients involved in energy metabolism in hopes of adding to the lab's accumulating evidence that pharmacological inhibition of nutrient transporters might represent an important toxicological mechanism in the nursing mother-neonate dyad.

The Caco-2, (human colorectal adenocarcinoma) cell line was chosen to represent the neonatal intestinal epithelium. This cell line displays a number of properties characteristic of differentiated intestinal epithelial cells (89). Good correlation has been identified for absorption of drugs in human jejunum and Caco-2 cells, especially for passively absorbed drugs (90, 91). Further, various transporters (including MCT1 an OCTN2), enzymes, and nuclear receptors expressed in the *in vivo* intestinal epithelium are present in the Caco-2 cells (91). These polarized epithelial cells have routinely been cultivated into polarized monolayers to study transepithelial transport of drugs across the intestinal epithelium, including studies done in our laboratory (83, 92). However, limitations and differences exist as this cell line is colorectal in nature and nutrient absorption typically occurs along the length of the small intestine. Furthermore, Caco-2 cells better represent the differentiated adult epithelium, while important differences in enzyme and transporter expression exist in the neonatal epithelium that often make extrapolation of information obtained in adult systems to the developing infant somewhat erroneous. For drugs absorbed primarily paracellularly or by transporters, the apparent permeability will be lower in Caco-2 cells due to narrower tight junctions and a reduced expression of absorptive transporters versus those found in the jejunum (91). Despite this, the use of the Caco-2 monolayer remains prevalent for permeability, transport, and metabolic studies due

to its well characterization and ability to maintain in culture (91). Therefore, we accepted the limitations and made use of the Caco-2 cell line to represent the neonatal intestinal epithelium in this proof of concept study.

When studying the polarized mammary epithelium, few *in vitro* models are available and include the CIT 3/fibrocyte co-culture (murine model) (93) and Mac-T cells (bovine model) (94). Recently, research groups have shown success using the BME-UV cells to represent a polarized monolayer of the mammary epithelium and have shown this cell line expresses the functional transporters of interest (86, 87). Unfortunately, I encountered problems culturing the cell line into a polarized monolayer in our home laboratory. I attempted to optimize media pH, frequency of media change, cell seeding density, duration of growth period, and transwell diameter. Despite my troubleshooting efforts, reaching a TEER value above 300 Ω was inconsistent and LY yellow rejection rates peaked at 85%, a clear indication that the cells did not form a polarized monolayer. Inability to form a polarized epithelium is a problem for two reasons; 1) it is well known tight junctions regulate gene expression. Without proper tight junction formation the cellular phenotype is unlikely to mimic the lactating epithelium *in vivo* (95, 96); and 2) this precluded an assessment of nutrient flux since both paracellular and transcellular transport routes were available for nutrient transfer across the epithelium. Assessment of flux was a main objective of the project. This forced the project to focus on the indirect effects of pharmacological inhibition of the nutrient transporters on barrier integrity through a disruption in cellular homeostasis.

The first step taken to evaluate the indirect effects was to assess barrier integrity by measuring TEER values and LY rejection rates. TEER measurements are used to measure the ion movement across the paracellular pathway of the epithelium and are used as an indirect assessment of tight junction establishment. LY is a substance that can only transverse the epithelium via the paracellular route, so similarly, it also depicts the 'tightness' of the tight junctions and integrity of the system. Their simultaneous measurement allows for a greater confidence in the determination of the integrity and polarization of the monolayer. On three separate occasions, cell lines were cultured for three weeks in 24 well transwells and exposed to IC_{50} values of known inhibitors to OCTN2, the high affinity transporter for L-carnitine uptake, and MCT1, the principle transporter involved in butyrate uptake, for 6, 12, and 24 hours as well as for 7 days, to represent acute and chronic inhibition, with TEER values and LY rejection rates

measured at each time point. No significant variation was noted between control and treatment groups in either cell line. One plausible explanation could be incomplete inhibition of the nutrient transport. While OCTN2 and MCT1 are high affinity L-carnitine and butyrate transporters, respectively, these nutrients are additionally transported by a variety of other transporters (9, 54, 82). The inhibitors chosen, verapamil and AR-C155858, were inhibitors specific of OCTN2 and MCT1, respectively. Therefore, L-carnitine and butyrate uptake into the epithelium may have been adequate to prevent any significant effects on barrier integrity. General inhibitors of L-carnitine and butyrate uptake transporters would be necessary to corroborate these suppositions, and further, to provide experimental support for the hypothesis.

Chronic exposure to drugs that inhibit transporter function is known to cause alteration in the expression of transporters (97, 98). To assess alterations in transporter expression profiles with chronic exposure to specific inhibitors of OCTN2 and butyrate, cells assessed for of TEER and LY rejection rates were subsequently washed with phosphate buffered saline and Trizol was added to allow cell lysis to occur. The sample was then collected and stored at -80°C until RNA extraction. Sufficient RNA yields were a concern with the use of 24-well transwells due to their minimal growing surface area. The low RNA yields, which averaged around 50 ng/µL, was likely due to an inadequate surface area cell growth, although RNA degradation due to cell storage cannot be ruled out. To address the low RNA yield, I made use of the SuperScript VILO cDNA synthesis kit. This kit is quite sensitive and I omitted the option of performing a 20-fold dilution of the resulting cDNA in hopes of obtaining the maximum cDNA concentration from the RNA yield. Unfortunately, qPCR confirmed the low RNA yields as C_T values of the internal control gene were quite high and the C_T values of the target genes were insufficient to allow their quantification under the present qPCR cycle conditions.

The second objective focused on the indirect effects of inhibition of L-carnitine and butyrate uptake on cellular homeostasis. Both L-carnitine and butyrate have key roles in the cellular energy metabolism and homeostasis. L-carnitine is essential for the utilization of long chain fatty acids (LCFAs) as it facilitates their transport into the mitochondrial matrix where the enzymes required for β-oxidation of LCFAs are located (69). Therefore, adequate concentrations of L-carnitine must exist in the tissues or β-oxidation will decrease and cellular energy metabolism will be impaired (69). Further, L-carnitine serves a key role in the activation of aerobic glycolysis, enhancement of respiratory chain function, donor of acetyl groups for

biosynthesis (e.g. acetyl choline), and membrane stabilization (68). Butyrate, acetate, and propionate, the predominant SCFAs, are absorbed readily by colonocytes and are used as the preferred source of fuel by these cells (75). Butyrate is oxidized more readily than propionate and acetate by colonocytes and its oxidation occurs regardless of the presence of other SCFAs (76). Due to this, β-oxidation of butyrate accounts for up to 70% of the totally energy consumed by the colonocytes (77). Due to the importance of these two nutrients in energy metabolism, any inhibition has the potential to alter cellular homeostasis resulting in disruption of the epithelial barrier. Further, adequate energy generation is critical to the maintenance of tight junction function (99). Therefore, inhibition of L-carnitine and/or butyrate can impact the integrity of the epithelium through either disruption of cellular homeostasis or through decreased tight junction function.

To assess the effects of pharmacological inhibition of L-carnitine and butyrate transporters on cellular homeostasis, focus was given to ATP production, glycolysis rates, and cellular respiration as a combined measurement of these parameters allows a detailed metabolic assessment (100-102). The main energy producing pathways within a cell, including glycolysis and β-oxidation of fatty acids, work in concert to maintain optimal cellular energy status (100). ATP levels in healthy cells are, therefore, maintained at a constant level (usually around 1-10 mM depending on the cell) (103). Parallel measurement of ECA fluxes and OCR, with measurement of ATP production, allows for a complete, systematic bioenergetics assessment within the cellular system (100). Three assays were selected; the CellTiter-Glo Luminescent Cell Viability Assay, the pH-Xtra Glycolysis Assay, and the MitoXpress Xtra Oxygen Consumption Assay to assess the above mentioned parameters, respectively.

The CellTiter-Glo Luminescent Cell Viability Assay determines the number of viable cells based on ATP quantitation which is directly proportional to the luminescent signal. Cells were seeded and allowed to attach prior to their treatment for 6 hours with the IC_{50} value of the chosen inhibitors. No significant variation in ATP content was found between the treated and control groups in either cell lines. This could be due to an inadequate duration of treatment where the breakdown of barrier integrity takes place chronically and requires consistent disruption of cellular homeostasis (104). In order to perform chronic studies, the cells require frequent media changes to prevent apoptosis as well as daily treatment with the inhibitors. Unfortunately, this was not possible for this assay as it is performed in 96 well plates and the

possibility of disrupting the cells is too great. Another plausible explanation could be the adaptation of the cells to the inhibition of butyrate and L-carnitine uptake. Both of these nutrients are critical for the oxidation of the fatty acids; L-carnitine is responsible for the transport of the fatty acid into the mitochondrial matrix and butyrate is the primary SCFA oxidized for energy within the intestine. When inhibited, the cells must adapt and generate their energy through other means or else apoptosis will occur. Often, and in the case of the mammary and intestinal epithelium, the secondary means of energy metabolism is through glycolysis.

As lactate is the main contributor to ECA, measuring ECA is a convenient way to assess cellular glycolytic flux. The pH-Xtra Glycolysis Assay allows for the real time, kinetic analysis of ECA, thus giving an insight into glycolytic activity. Cells were seeded at 50,000 cells/well as the assay suggested this density would provide a suitable balance between ECA response and cell availability. Optional controls for this assay included a signal control, blank control, positive control (Antimycin A) and negative control (Oxamic Acid). The first three of the optional controls were utilized. Cells were allowed to attach overnight before being exposed to the inhibitors. Kinetic analysis of ECA was measured immediately for 120 minutes. In treatments with both verapamil and AR-C155858, an upward trend in glycolytic flux was noted in both the Caco-2 and BME cell lines. This is consistent with the expected results as both L-carnitine and butyrate are required for the β-oxidation of fatty acids in the production of energy. When inhibited, the cells adapt and switch to glycolysis in order to obtain the necessary energy. Cell survival is dependent on stimulating glucose oxidation, either directly or indirectly, when fatty acid oxidation is inhibited (105). Liepinsh et al. found a substantial increase in rate of glucose uptake when L-carnitine concentration was reduced by mildronate treatment and suggested that the change in glucose metabolism represented a compensatory role (106). It was expected, however, to have seen a greater increase in glycolysis in the Caco-2 cell line as the intestinal epithelium relies on β-oxidation of fatty acids as its preferred energy source, while the mammary epithelium relies on glycolysis. This could be explained by incomplete inhibition of the MCT1 transporter resulting in continued fatty acid oxidation as an energy source. Use of the negative control would have provided further insight towards this as the level of increased glycolytic flux we observed could have been compared to the negative response. This would have confirmed the response we were seeing as, in fact, an upward trend.

The MitoXpress Oxygen Consumption Assay allows for the kinetic analysis of cellular respiration by measuring extracellular oxygen consumption. Optional controls for this assay included a signal control, blank control, negative control (Antimycin A) and positive control (Glucose Oxidase). The first three of the optional controls were utilized. Cells were allowed to attach overnight before being exposed to the inhibitors. Kinetic analysis of OCR was measured immediately for 120 minutes. In treatments with both verapamil and AR-C155858, an upward trend in cellular respiration was noted in both the Caco-2 and BME cell lines. With an increase in glycolysis, one would expect to see a decrease in oxygen consumption. Alcorn et al found up to a 75% reduction in respiration in the presence of D-lactate, an inhibitor of transport by MCTs (88). L-Lactate, when transported into the mitochondria by MCTs, is metabolized to pyruvate for energy metabolism (88). Similar findings should have been noted with the inhibition of MCT transport of butyrate; however, we noted an upward trend in respiration. One explanation to this increase could be the production of reactive oxygen species (ROS). Neutrophils, in particular, have been shown to undergo a 'respiratory burst' and generate substantial amounts of ROS under numerous circumstances including transporter inhibition (107). This occurs through activation of the NADPH-oxidase system, which in turn, catalyzes oxygen molecules to form superoxide anions during non-mitochondria oxygen uptake (107). These reactive oxidant superoxides are then converted to hydrogen peroxide which is metabolized into oxygen and water, oxidized glutathione and water, or the more potent hydroxyl radicals (107). The superoxides as well as the radicals can both elucidate an inflammatory response as well as mediate cell death (107). Maintaining a high butyrate concentration in the colon has been related to a reduction in ROS-induced injury of colonocytes (107). Therefore, inhibition of MCT1, the main transporter of butyrate, could potentially lead to an increase in ROS production resulting in an increase in oxygen consumptions noted in our experiments.

In summary, our study attempted to provide a proof-of-concept for the ability of drug-nutrient transporter interactions at mammary and intestinal epithelia to directly and indirectly affect the developing neonate. Inhibition of the flux of essential nutrients across the barrier may result in a decrease in the availability of these key components that are essential for proper growth and maturation of the developing neonate. Due to the importance of these nutrients on epithelial cellular energy metabolism this, indirectly, has the ability to disrupt barrier integrity through a loss of cellular homeostasis. Epithelial dysfunction may lead to adverse effects on the

neonate. Complications in obtaining a polarized mammary monolayer forced my thesis work to focus on the indirect affects which were measured by assessing barrier integrity and cellular homeostasis. No change was noted upon treatment with MCT1 and OCTN2 inhibitors on TEER values, LY rejection rates, or ATP production. Upward trends were noted in treatment groups in glycolytic flux and oxygen consumption in both cell lines. Overall, pharmacological inhibition of the high affinity transporters of L-carnitine and butyrate had no significant effect on epithelial cellular functions as reflected through glycolytic flux, oxygen consumption rates, and ATP production.

6. FUTURE WORK

A main focus of this study was the assessment of the direct effects of pharmacological inhibition of nutrient transporters at the mammary and intestinal epithelium on nutrient flux and the indirect effect of inhibition on the integrity of these polarized epithelia. To assess this, it was critical to achieve a polarized monolayer of both systems to allow for the comparison between the mammary and intestinal epithelia. Unfortunately, this was not achieved with the experimental system chosen to represent the mammary epithelium, the BME-UV cell line, despite literature evidence to the contrary. Obtaining and validating a polarized mammary epithelium is critical in advancing our understanding of the direct and indirect effects of pharmacological inhibition of nutrient transporters on nutrient flux and epithelial barrier function.

Challenges exist when selecting an *in vitro* system to represent the mammary and intestinal polarized epithelia. Few *in vitro* models exist although significant recent advances in alternate experimental systems such as tissue explants, 3D cultures, organoids, and primary epithelial cells, make such systems an attractive alternative to assess my research hypotheses. These alternative systems warrant attention as the currently used, 2D filter insert culture system is expensive, laborious and requires large numbers of cells per sample. Further, they fail to accurately represent the complex and active nature of the mammary and intestinal epitheliums that exist *in vivo.*

In particular, future studies should make use of 3D cultures (possibly those created from primary epithelial cells) to represent the mammary and intestinal epithelia. Such 3D culture systems have drastically evolved since their conception and continue to undergo important refinements that aim to ultimately recreate the organ in culture (108). Furthermore, it will potentially allow investigations pertaining to particular development stages and environmental constraints that exist in the *in vivo* system (108). This is of particular importance when examining dynamic systems such as that of the lactating mammary and neonatal intestinal epithelia as both go under a great amount of growth and differentiation over time.

To set up a 3D culture, the epithelial cells are cultured inside Laminin-Rich Extracellular Matrix (lrECM) such that they are fully surrounded by an lrECM thick coat (108). Biochemical analysis, including RNA profiling and quantitation as well as protein analysis, is possible with

3D cultures and is usually done by solubilizing the gels using ECM-specific proteases (ex: PBS-EDTA) (108). The extracted cells are then subjected to the protocols normally made use of for RNA extraction and isolation. This not only allows insight into transporter expression, but can also be used to assess the proteins associated with tight junction formation. Tight junctions are integrated by numerous proteins including occludin, tricellulin, claudins and JAMS which represent the integral proteins and are all responsible for paracellular ionic selectivity (95). Further proteins, the adapter proteins, include ZOs, MAGIs, cingulin and paracingulin and function as the bridge between the integral proteins and the actin cytoskeleton (95). Tight junction formation is critical for barrier integrity, cellular energy metabolism and gene expression; therefore, assessing the quantitation of the proteins involved in tight junction formation allows insight into the effects of pharmacological inhibition of nutrient transporters on epithelial function (104).

One of the most critical studies when assessing pharmacological inhibition of transporters is looking at the flux of the nutrients associated with the transporters you are inhibiting. This is challenging due to the time dependence of such studies, in particular, with butyrate as it is oxidized in the system so readily. However, these studies are invaluable when assessing the direct effects of nutrient transporter inhibition. Radiolabeled tracers can provide insightful information on the flux distributions within biological samples. Intracellular fluxes can be directly determined from the radioactivity count data by tracking the depletion of the radiolabeled metabolite and/or the accompanying accumulation of any products formed (109). For example, ^{13}C-labelling can yield flux information within bacterial cultures, mammalian cell culture, organ tissues and erythrocytes (109). By assessing the flux of the nutrients involved in energy metabolism, it allows insight on the degree of pharmacological inhibition and the direct effects of such inhibition on the cell.

In summary, obtaining and utilizing a more accurate portrayal of the lactating mammary and neonatal intestinal epithelium is critical in answering this research question. 3D cultures provide promise for this as they allow investigations pertaining to particular development stages and environmental constraints, which is critical when examining the two epithelial systems. Assessment of the flux of the essential nutrients is key to understanding the direct effects of pharmacological inhibition of transporters. Finally, assessment of the alterations of tight

junction function following nutrient transporter inhibition warrant attentions as tight junctions are critical for barrier integrity, cellular homeostasis, and gene expression.

7. REFERENCES

1. Ballard O, Morrow AL. Human milk composition: nutrients and bioactive factors. Pediatr Clin North Am. 2013;60(1):49-74.
2. Walker A. Breast milk as the gold standard for protective nutrients. J Pediatr. 2010;156(2):S3-S7.
3. Donovan SM. Role of human milk components in gastrointestinal development: current knowledge and future needs. J Pediatr. 2006;149(5):S49-S61.
4. Neville MC, Allen JC, Archer PC, Casey CE, Seacat J, Keller RP, et al. Studies in human lactation: milk volume and nutrient composition during weaning and lactogenesis. Am J Clin Nut. 1991;54(1):81-92.
5. Lewis-Jones DI, Lewis-Jones MS, Connolly RC, Lloyd DC, West CR. Sequential changes in the antimicrobial protein concentrations in human milk during lactation and its relevance to banked human milk. Pediatr Res. 1985;19(6):561-5.
6. Neville MC, Keller R, Seacat J, Lutes V, Neifert M, Casey C, et al. Studies in human lactation: milk volumes in lactating women during the onset of lactation and full lactation. Am J Clin Nut. 1988;48(6):1375-86.
7. Liao Y, Alvarado R, Phinney B, Lönnerdal B. Proteomic characterization of human milk whey proteins during a twelve-month lactation period. J Proteome Res. 2011;10(4):1746-54.
8. Nommsen LA, Lovelady CA, Heinig MJ, Lönnerdal B, Dewey KG. Determinants of energy, protein, lipid, and lactose concentrations in human milk during the first 12 mo of lactation: the DARLING Study. Am J Clin Nutr. 1991;53(2):457-65.
9. Ling B, Alcorn J. Acute administration of cefepime lowers L-carnitine concentrations in early lactation stage rat milk. J Nutr. 2008;138(7):1317-22.
10. Gilchrist SE, Alcorn J. Lactation stage-dependent expression of transporters in rat whole mammary gland and primary mammary epithelial organoids. Fundam Clin Pharmacol. 2010;24(2):205-14.
11. Gomez HF, Ochoa TJ, Carlin LG, Cleary TG. Human lactoferrin impairs virulence of Shigella flexneri. J Infect Dis. 2003;187(1):87-95.

12. Lima MF, Kierszenbaum F. Lactoferrin effects of phagocytic cell function. II. The presence of iron is required for the lactoferrin molecule to stimulate intracellular killing by macrophages but not to enhance the uptake of particles and microorganisms. J Immunol. 1987;139(5):1647-51.
13. Harmsen MC, Swart PJ, de Béthune M-P, Pauwels R, De Clercq E, Meijer DKF. Antiviral effects of plasma and milk proteins: lactoferrin shows potent activity against both human immunodeficiency virus and human cytomegalovirus replication in vitro. J Infect Dis. 1995;172(2):380-8.
14. Thormar H, Isaacs CE, Brown HR, Barshatzky MR, Pessolano T. Inactivation of enveloped viruses and killing of cells by fatty acids and monoglycerides. Antimicrob Agents Chemother. 1987;31(1):27-31.
15. Hanson L. Comparative immunological studies of the immune globulins of human milk and of blood serum. Int Arch Allergy and Immunol. 1961;18(5):241-67.
16. Koletzko B, Rodriguez-Palmero M, Demmelmair H, Fidler N, Jensen R, Sauerwald T. Physiological aspects of human milk lipids. Early Hum Develop. 2001;65:S3-S18.
17. Picciano MF. Nutrient composition of human milk. Pediatr Clin North Am. 2001;48(1):53-67.
18. Ashworth CJ, Antipatis C. Micronutrient programming of development throughout gestation. Reproduction. 2001;122(4):527-35.
19. Epstein FH, Fish EM, Molitoris BA. Alterations in epithelial polarity and the pathogenesis of disease states. N Engl J Med. 1994;330(22):1580-8.
20. Bryant DM, Mostov KE. From cells to organs: building polarized tissue. Nat Rev Mol Cell Bio. 2008;9(11):887-901.
21. Anderson JM. Molecular structure of tight junctions and their role in epithelial transport. Physiol. 2001;16(3):126-30.
22. Semenza GL. Regulation of oxygen homeostasis by hypoxia-inducible factor 1. Physiol. 2009;24(2):97-106.
23. McManaman JL, Neville MC. Mammary physiology and milk secretion. Adv Drug Deliv Rev. 2003;55(5):629-41.
24. Abraham S, Hirsch PF, Chaikoff IL. The quantitative significance of glycolysis and non-glycolysis in glucose utilization by rat mammary gland. J Bio Chem. 1954;211(1):31-8.

25. Neville MC. Milk Secretion: An Overview. 1998.
26. Hollmann KH. Cytology and fine structure of the mammary gland. Lactation A Comprensive Treatise BL Larson & VR Smith, eds. 1974.
27. Neville MC, Morton J, Umemura S. Lactogenesis: the transition from pregnancy to lactation. Pediatr Clin North Am. 2001;48(1):35-52.
28. Kuhn NJ, Peaker M. Lactogenesis: the search for trigger mechanisms in different species. UK, Zool Soc London: Comparative aspects of lactation. 1977:165-92.
29. Neville MC, McFadden TB, Forsyth I. Hormonal regulation of mammary differentiation and milk secretion. J Mammary Gland Biol Neoplasia. 2002;7(1):49-66.
30. Shennan DB, Peaker M. Transport of milk constituents by the mammary gland. Physiolog Rev. 2000;80(3):925-51.
31. Linzell JL, Mepham TB, Peaker M. The secretion of citrate into milk. J Physiol. 1976;260(3):739-50.
32. Fasano A, Shea-Donohue T. Mechanisms of disease: the role of intestinal barrier function in the pathogenesis of gastrointestinal autoimmune diseases. Nat Clin Practice Gastroenterol Hepatol. 2005;2(9):416-22.
33. Clayburgh DR, Shen L, Turner JR. A porous defense: the leaky epithelial barrier in intestinal disease. Lab Invest. 2004;84(3):282-91.
34. Scheppach W. Effects of short chain fatty acids on gut morphology and function. Gut. 1994;35(1 Suppl):S35-S8.
35. Ruppin H, Bar-Meir S, Soergel KH, Wood C, Schmitt Jr MG. Absorption of short-chain fatty acids by the colon. Gastroenterol. 1980;78(6):1500-7.
36. Fleming SE, Zambell KL, Fitch MD. Glucose and glutamine provide similar proportions of energy to mucosal cells of rat small intestine. Am J Physiol Gastrointestl Liver Physiol. 1997;273(4):G968-G78.
37. Neville MC, Anderson SM, McManaman JL, Badger TM, Bunik M, Contractor N, et al. Lactation and neonatal nutrition: defining and refining the critical questions. J Mammary Gland Biol Neoplasia. 2012;17(2):167-88.
38. Chipponi JX, Bleier JC, Santi MT, Rudman D. Deficiencies of essential and conditionally essential nutrients. Am J Clin Nutr. 1982;35(5):1112-6.

39. Grimble GK. Essential and conditionally-essential nutrients in clinical nutrition. Nutr Res Rev. 1993;6(01):97-119.
40. Ho RH, Kim RB. Drug Transporters. Handbook of Drug-Nutrient Interactions: Springer; 2010. p. 45-84.
41. Eckford PDW, Sharom FJ. ABC efflux pump-based resistance to chemotherapy drugs. Chem Rev. 2009;109(7):2989-3011.
42. Schinkel AH, Jonker JW. Mammalian drug efflux transporters of the ATP binding cassette (ABC) family: an overview. Adv Drug Deliv Rev. 2003;55(1):3-29.
43. Dean M, Hamon Y, Chimini G. The human ATP-binding cassette (ABC) transporter superfamily. J Lip Res. 2001;42(7):1007-17.
44. He L, Vasiliou K, Nebert DW. Analysis and update of the human solute carrier (SLC) gene superfamily. Hum Genomics. 2009;3(2):195.
45. Fredriksson R, Nordström KJV, Stephansson O, Hägglund MGA, Schiöth HB. The solute carrier (SLC) complement of the human genome: phylogenetic classification reveals four major families. FEBS Lett. 2008;582(27):3811-6.
46. Haitina T, Lindblom J, Renström T, Fredriksson R. Fourteen novel human members of mitochondrial solute carrier family 25 (SLC25) widely expressed in the central nervous system. Genomics. 2006;88(6):779-90.
47. Visser WF, Van Roermund CWT, Waterham HR, Wanders RJA. Identification of human PMP34 as a peroxisomal ATP transporter. Biochem Biophys Res Commun. 2002;299(3):494-7.
48. Takamori S. VGLUTs:'exciting'times for glutamatergic research? Neurosci Res. 2006;55(4):343-51.
49. Tamai I, Yabuuchi H, Nezu J-i, Sai Y, Oku A, Shimane M, et al. Cloning and characterization of a novel human pH-dependent organic cation transporter, OCTN1. FEBS Lett. 1997;419(1):107-11.
50. Tamai I, Ohashi R, Nezu J-i, Yabuuchi H, Oku A, Shimane M, et al. Molecular and functional identification of sodium ion-dependent, high affinity human carnitine transporter OCTN2. J Biol Chem. 1998;273(32):20378-82.
51. Ito S, Alcorn J. Xenobiotic transporter expression and function in the human mammary gland. Adv Drug Deliv Rev. 2003;55(5):653-65.

52. Ohashi R, Tamai I, Nezu J-i, Nikaido H, Hashimoto N, Oku A, et al. Molecular and physiological evidence for multifunctionality of carnitine/organic cation transporter OCTN2. Mol Pharmacol. 2001;59(2):358-66.
53. Ohashi R, Tamai I, Inano A, Katsura M, Sai Y, Nezu J-i, et al. Studies on functional sites of organic cation/carnitine transporter OCTN2 (SLC22A5) using a Ser467Cys mutant protein. J Pharmacol Exp Ther. 2002;302(3):1286-94.
54. Ritzhaupt A, Wood IS, Ellis A, Hosie KB, Shirazi-Beechey SP. Identification and characterization of a monocarboxylate transporter (MCT1) in pig and human colon: its potential to transport l-lactate as well as butyrate. J Physiol. 1998;513(3):719-32.
55. Thibault R, De Coppet P, Daly K, Bourreille A, Cuff M, Bonnet C, et al. Down-regulation of the monocarboxylate transporter 1 is involved in butyrate deficiency during intestinal inflammation. Gastroenterol. 2007;133(6):1916-27.
56. Chan L-N. Drug-nutrient interactions. J Parenteral Enteral Nutr. 2013:0148607113488799.
57. Peng L, He Z, Chen W, Holzman IR, Lin J. Effects of butyrate on intestinal barrier function in a Caco-2 cell monolayer model of intestinal barrier. Pediatr Res. 2007;61(1):37-41.
58. Stieger B, Fattinger K, Madon J, Kullak-Ublick GA, Meier PJ. Drug-and estrogen-induced cholestasis through inhibition of the hepatocellular bile salt export pump (Bsep) of rat liver. Gastroenterol. 2000;118(2):422-30.
59. Tsuji A. Transporter-mediated drug interactions. Drug Metab Pharmacokinet. 2002;17(4):253-74.
60. Neville MC, Walsh CT. Effects of xenobiotics on milk secretion and composition. Am J Clin Nutr. 1995;61(3):687S-94S.
61. Ito S, Lee A. Drug excretion into breast milk—overview. Adv Drug Deliv Rev. 2003;55(5):617-27.
62. Wu X, Huang W, Prasad PD, Seth P, Rajan DP, Leibach FH, et al. Functional characteristics and tissue distribution pattern of organic cation transporter 2 (OCTN2), an organic cation/carnitine transporter. J Pharmacol Exp Ther. 1999;290(3):1482-92.
63. Plagemann A, Harder T, Franke K, Kohlhoff R. Long-term impact of neonatal breast-feeding on body weight and glucose tolerance in children of diabetic mothers. Diabetes care. 2002;25(1):16-22.

64. Thibault R, Blachier F, Darcy-Vrillon B, de Coppet P, Bourreille A, Segain JP. Butyrate utilization by the colonic mucosa in inflammatory bowel diseases: a transport deficiency. Inflamm Bowel Dis. 2010;16(4):684-95.
65. McKenna MC, Hopkins IB, Carey A. α-cyano-4-hydroxycinnamate decreases both glucose and lactate metabolism in neurons and astrocytes: Implications for lactate as an energy substrate for neurons. J Neurosci Res. 2001;66(5):747-54.
66. Halestrap AP, Denton RM. Specific inhibition of pyruvate transport in rat liver mitochondria and human erythrocytes by α-cyano-4-hydroxycinnamate. Biochem J. 1974;138(2):313.
67. Rovamo LM, Salmenperä L, Arjomaa P, Raivio KO. Carnitine during prolonged breast feeding. Pediatr Res. 1986;20(8):806-9.
68. Arenas Jn, Rubio JC, Martín MA, Campos Y. Biological roles of L-carnitine in perinatal metabolism. Early Hum Develop. 1998;53:S43-S50.
69. Borum PR. Carnitine. Annual review of nutrition. 1983;3(1):233-59.
70. Knapp AC, Todesco L, Török M, Beier K, Krähenbühl S. Effect of carnitine deprivation on carnitine homeostasis and energy metabolism in mice with systemic carnitine deficiency. Ann Nutr Metab. 2008;52(2):136-44.
71. Lamhonwah A-M, Mai L, Chung C, Lamhonwah D, Ackerley C, Tein I. Upregulation of mammary gland OCTNs maintains carnitine homeostasis in suckling infants. Biochem Biophys Res Commun. 2011;404(4):1010-5.
72. Di Donato S. Disorders of lipid metabolism affecting skeletal muscle: Carnitine deficiency syndromes, defects in the catabolic pathway, and chanarin disease. Myol. 1994;2:1587-609.
73. Novak M, Monkus EF, Chung D, Buch M. Carnitine in the perinatal metabolism of lipids I. Relationship between maternal and fetal plasma levels of carnitine and acylcarnitines. Pediatr. 1981;67(1):95-100.
74. Battistella PA, Vergani L, Donzelli F, Rubaltelli FF, Angelini C. Plasma and urine carnitine levels during development. Pediatr Res. 1980;14(12):1379-81.
75. Bugaut M. Occurrence, absorption and metabolism of short chain fatty acids in the digestive tract of mammals. Comp Biochem Physiol B Comp Biochem. 1987;86(3):439-72.

76. Clausen MR, Mortensen PB. Kinetic studies on the metabolism of short-chain fatty acids and glucose by isolated rat colonocytes. Gastroenterol Baltimore Then Philadelphia. 1994;106:423-.
77. Hague A, Butt AJ, Paraskeva C. The role of butyrate in human colonic epithelial cells: an energy source or inducer of differentiation and apoptosis? Proc Nutr Soc. 1996;55(03):937-43.
78. Niles RM, Wilhelm SA, Thomas P, Zamcheck N. The effect of sodium butyrate and retinoic acid on growth and CEA production in a series of human colorectal tumor cell lines representing different states of differentiation. Cancer Invest. 1988;6(1):39-45.
79. Hodin RA, Meng S, Archer S, Tang R. Cellular growth state differentially regulates enterocyte gene expression in butyrate-treated HT-29 cells. Cell Growth Diff. 1996;7(5):647-53.
80. Meng S, Wu JT, Archer SY, Hodin RA. Short-chain fatty acids and thyroid hormone interact in regulating enterocyte gene transcription. Surgery. 1999;126(2):293-8.
81. Borthakur A, Saksena S, Gill RK, Alrefai WA, Ramaswamy K, Dudeja PK. Regulation of monocarboxylate transporter 1 (MCT1) promoter by butyrate in human intestinal epithelial cells: Involvement of NF-κB pathway. J Cell Biochem. 2008;103(5):1452-63.
82. Hadjiagapiou C, Schmidt L, Dudeja PK, Layden TJ, Ramaswamy K. Mechanism (s) of butyrate transport in Caco-2 cells: role of monocarboxylate transporter 1. Am J Physiol Gastrointest Liver Physiol. 2000;279(4):G775-G80.
83. Artursson P, Palm K, Luthman K. Caco-2 monolayers in experimental and theoretical predictions of drug transport. Adv Drug Deliv Rev. 2012;64:280-9.
84. Quesnell RR, Erickson J, Schultz BD. Apical electrolyte concentration modulates barrier function and tight junction protein localization in bovine mammary epithelium. Am J Physiol Cell Physiol. 2007;292(1):C305-C18.
85. Englund G, Rorsman F, Rönnblom A, Karlbom U, Lazorova L, Gråsjö J, et al. Regional levels of drug transporters along the human intestinal tract: co-expression of ABC and SLC transporters and comparison with Caco-2 cells. Eur J Pharml Sci. 2006;29(3):269-77.
86. Al-Bataineh MM, Van Der Merwe D, Schultz BD, Gehring R. Cultured mammary epithelial monolayers (BME-UV) express functional organic anion and cation transporters. J Vet Pharmacol Ther. 2009;32(5):422-8.

87. Schmidt CR, Carlin RW, Sargeant JM, Schultz BD. Neurotransmitter-stimulated ion transport across cultured bovine mammary epithelial cell monolayers. J Dairy Sci. 2001;84(12):2622-31.
88. Ling B, Peng F, Alcorn J, Lohmann K, Bandy B, Zello GA. D-Lactate altered mitochondrial energy production in rat brain and heart but not liver. Nutr Metab. 2012;9(6):b25.
89. Rousset M. The human colon carcinoma cell lines HT-29 and Caco-2: two in vitro models for the study of intestinal differentiation. Biochim. 1986;68(9):1035-40.
90. Yee S. In vitro permeability across Caco-2 cells (colonic) can predict in vivo (small intestinal) absorption in man—fact or myth. Pharm Res. 1997;14(6):763-6.
91. Sun H, Chow ECY, Liu S, Du Y, Pang KS. The Caco-2 cell monolayer: usefulness and limitations. 2008.
92. Mukker JK, Michel D, Muir AD, Krol ES, Alcorn J. Permeability and Conjugative Metabolism of Flaxseed Lignans by Caco-2 Human Intestinal Cells. J Nat Prod. 2014;77(1):29-34.
93. Toddywalla VS, Kari FW, Neville MC. Active transport of nitrofurantoin across a mouse mammary epithelial monolayer. J Pharmacol Exp Ther. 1997;280(2):669-76.
94. Huynh HT, Robitaille G, Turner JD. Establishment of bovine mammary epithelial cells (MAC-T): an in vitro model for bovine lactation. Exp Cell Res. 1991;197(2):191-9.
95. González-Mariscal L, Domínguez-Calderón A, Raya-Sandino A, Ortega-Olvera JM, Vargas-Sierra O, Martínez-Revollar G, editors. Tight junctions and the regulation of gene expression2014: Elsevier.
96. Bordin M, D'Atri F, Guillemot L, Citi S. Histone Deacetylase Inhibitors Up-Regulate the Expression of Tight Junction Proteins11Swiss Cancer League, Swiss National Science Foundation, Ministry for Italian University and Research, ERASMUS Program (M. Bordin), and Roche Research Foundation fellowship (L. Guillemot). Mol Cancer Res. 2004;2(12):692-701.
97. Huang H, Liu N, Yang C, Liao S, Guo H, Zhao K, et al. HDAC inhibitor L-carnitine and proteasome inhibitor bortezomib synergistically exert anti-tumor activity in vitro and in vivo. PloS One. 2012;7(12):e52576.

98. Davie JR. Inhibition of histone deacetylase activity by butyrate. J Nutr. 2003;133(7):2485S-93S.
99. Madara JL, Moore R, Carlson S. Alteration of intestinal tight junction structure and permeability by cytoskeletal contraction. Am J Physiol Cell Physiol. 1987;253(6):C854-C61.
100. Papkovsky DB, Zhdanov AV. Cell Energy Budget Platform for Assessment of Cell Metabolism. Mitochondrial Medicine: Volume II, Manipulating Mitochondrial Function. 2015:333-48.
101. Zhdanov AV, Waters AHC, Golubeva AV, Dmitriev RI, Papkovsky DB. Availability of the key metabolic substrates dictates the respiratory response of cancer cells to the mitochondrial uncoupling. Biochim Biophys Acta. 2014;1837(1):51-62.
102. Hynes J, O'Riordan TC, Zhdanov AV, Uray G, Will Y, Papkovsky DB. In vitro analysis of cell metabolism using a long-decay pH-sensitive lanthanide probe and extracellular acidification assay. Anal Biochem. 2009;390(1):21-8.
103. Beis I, Newsholme EA. The contents of adenine nucleotides, phosphagens and some glycolytic intermediates in resting muscles from vertebrates and invertebrates. Biochem J. 1975;152:23-32.
104. Fink MP, Delude RL. Epithelial barrier dysfunction: a unifying theme to explain the pathogenesis of multiple organ dysfunction at the cellular level. Crit Care Clin. 2005;21(2):177-96.
105. Lopaschuk GD. Optimizing cardiac energy metabolism: how can fatty acid and carbohydrate metabolism be manipulated? Coronary Artery Dis. 2001;12:S8-11.
106. Liepinsh E, Vilskersts R, Skapare E, Svalbe B, Kuka J, Cirule H, et al. Mildronate decreases carnitine availability and up-regulates glucose uptake and related gene expression in the mouse heart. Life Sci. 2008;83(17):613-9.
107. Liu Q, Shimoyama T, Suzuki K, Umeda T, Nakaji S, Sugawara K. Effect of sodium butyrate on reactive oxygen species generation by human neutrophils. Scand J Gastroenterol. 2001;36(7):744-50.
108. Mroue R, Bissell MJ. Three-dimensional cultures of mouse mammary epithelial cells. Epithelial Cell Culture Protocols: Springer; 2013. p. 221-50.

109. Yanagimachi KS, Stafford DE, Dexter AF, Sinskey AJ, Drew S, Stephanopoulos G. Application of radiolabeled tracers to biocatalytic flux analysis. Eur J Biochem. 2001;268(18):4950-60.